Title: MEG decoding reveals structural differences within integrative decision processes

Authors: Eran Eldar[1,2,*], Gyung Jin Bae[1,2], Zeb Kurth-Nelson[1,2], Peter Dayan[2,3,†], Raymond J. Dolan[1,2,†]

Affiliations

[1] Wellcome Trust Centre for Neuroimaging, University College London, London WC1N 3BG, UK

[2] Max Planck University College London Centre for Computational Psychiatry and Ageing Research, London WC1B 5EH, UK

[3] Gatsby Computational Neuroscience Unit, University College London, London W1T 4JG, UK

[†] These authors contributed equally to this work.

[*] Correspondence to: Eran Eldar

Wellcome Trust Centre for Neuroimaging

University College London

12 Queen Square, London WC1N 3BG, UK

Tel: +44 (0)20 3448 4362

Email: eran.eldar@mail.huji.ac.il

Main Text

When confronted with complex inputs consisting of multiple elements, humans employ various strategies to integrate the elements quickly and accurately. For instance, accuracy may be improved by processing elements one at a time[1–4] or over extended periods[5–8]; speed can increase if internal representation of elements are accelerated[9,10]. However, little is known about how humans actually approach these challenges, because behavioral findings can be accounted for by multiple alternative process models[11], and neuroimaging investigations typically rely on hemodynamic signals that change too slowly. Consequently, to uncover the fast neural dynamics that support information integration, we decoded magnetoencephalographic (MEG) signals recorded as human subjects performed a complex decision task. Our findings reveal three sources of individual differences in the temporal structure of subjects' integration processes – sequential representation, partial reinstatement, and early computation – each having a dissociable impact on how subjects handled problem complexity and temporal constraints. Our findings shed new light on the structure and influence of self-determined neural integration processes.

The neurophysiological processes that support information integration have been extensively studied[5–8]. However, in these studies elements of information are typically made available gradually over time, giving the experimenter control over what the subject processes at any given moment. In contrast, real life situations often require integration of complex information that is wholly available when the need to make a decision arises. Such situations pose an additional challenge to decision makers, requiring them to determine how to utilize time. For instance, one could opt to process multiple elements of information together or one after the other; elements could be stored in memory and then either fully or partially reinstated; and the decision process could be extended in time even if no new information is available. Here we ask whether people differ from one another in how these integration processes are structured. Additionally, we examine how such differences

relate to one's ability to tackle decision problems of varying complexity under varying time constraints.

For this purpose, we designed a class of information processing problems for which we could parametrically vary the complexity of the information that needs to be combined, as well as the time available for processing. We expected, and indeed found, that participants differ from one another in how they cope with these constraints. We used a computational model to capture these differences in terms of the values of particular parameters, which specified that there is latent order in the way that processing resources are divided among relevant stimuli. The modeled impact that division of resources had on an individual participant's calculations explained how their performance was affected by problem complexity and time constraints.

However, this model was couched at an abstract level, and could only provide limited information about how computations were realized. To gain insight into the temporal structure of participants' integration processes, we utilized recently developed methods for interpreting MEG signals that offer a substantially improved window onto the fast neural dynamics that humans employ when processing information and making decisions. In particular, recent work has employed MEG to reveal how representations of visual stimuli evolve over a timescale of tens of milliseconds[9–14], whether representations of distinct stimuli follow one another in time[15,16], and how decision variables evolve over time in simple decision making tasks[9,17]. These methods enabled us to decode MEG signals recorded as participants performed our task, providing direct access to the information subjects were processing at any moment in time.

General computational considerations and existing literature' suggest at least three structural dimensions of difference that can impact on how participants perform the task: treating stimuli in

series, one after the other, versus handling them in parallel[1–4]; complete versus partial encoding of stimuli[10]; and prolonged versus abbreviated processing[5–8]. Our findings indicate people differ from one another on all three dimensions, and this is reflected in how effective each person is at integrating information given different levels of problem complexity and time constraints.

To probe how people combine multiple elements of information under varying task constraints, we presented participants with a series of 'teams', each comprising up to four 'player' types present in varying numbers. Participants were asked to predict how many goals each team would score, based on pre-acquired explicit knowledge of the scoring ability of each player type (**Fig. 1**a,b; **Supplementary Fig. 1**). Across trials, we independently manipulated problem complexity (the numbers of player types in a given team) and available time (participants had either 1 or 2 seconds deliberation time before being prompted to report their prediction score quickly). Because participants could have arrived at approximate answers without actually distinguishing between players of different types (e.g., by relying on the total number of players), our initial analysis of task performance quantified how frequently participants provided precisely correct answers. Overall, task performance was better for less complex problems as well as when more time was available to form a decision (**Fig. 1**c). However, as expected, we observed substantial variation amongst participants in how problem complexity and available time impacted performance.

Firstly, many participants benefitted only slightly, or not at all, from the provision of additional time (**Fig. 1**d). To facilitate further analysis of these individual differences we divided participants into two groups ('time-sensitive' and 'time-insensitive'), using a median split on the degree to which a participant benefited from additional time ('2s minus 1s performance'). Complementary analyses examined linear relationships across the whole study sample. We found that the degree to which the time-sensitive group performed better on 2 s trials compared to 1 s trials was larger for

4

problems involving multiple types of player than for problem with single player type (permutation test: p = 0.02; M = 6.7%, 95% CI: 1.0 to 12.3), indicating these participants used additional time to manage greater problem complexity.

Secondly, participants exhibited a notable degree of individual differences in the extent to which their performance was affected by high problem complexity, especially when little time was available (i.e., in 1 sec trials). Here some participants' suffered a performance decrement that was more than three times as large as that of others (**Fig. 1**e). This individual variation in sensitivity to complexity in 1 sec trials (range: 28% to 89% performance decrement with 4 types compared to 1 type of player) correlated with the more limited individual variation in sensitivity to complexity evident with 2 second trial duration (robust estimation of regression coefficient for the z-scored measures, tested with random permutations: p = 0.014, β = 0.41, 95% CI: 0.08 to 0.73), indicating complexity sensitivity was to some degree stable across conditions.

Two linked observations suggest that participants' strategies reflected an underlying tradeoff associated with both time and complexity. First, individual variation in sensitivity to complexity was uncorrelated with overall performance in 1s trials (robust estimation of regression coefficient for the z-scored measures, tested with random permutations: p = 0.68, β = 0.08, 95% CI: –0.27 to 0.41), meaning that participants who did relatively better on the more complex trials did relatively worse on the simpler ones. Second, this effect was associated with a benefit participants gained from extra time. In other words, the worse a participant performed on the most complex problems (i.e., with 4 player types), when only 1 sec was available, the more they benefitted from extra time (robust estimation of regression coefficient for the z-scored measures, tested with random permutations: p = 0.01, β = 0.40, 95% CI: 0.09 to 0.72); equally, those whose performance was most sensitive to complexity were also those who benefitted most from additional time (**Fig. 1**f).

The behavioral observations reported above are informative about the general consequences of attempting to solve problems that are too difficult with too few computational resources and too little time. However, they do not exploit the information available in the precise errors that subjects made, and therefore offer limited insight into the strategies participants adopted. Errors can arise when participants ignore players, or perform calculations inaccurately. Therefore, we sought to build a model that offers a quantitative characterization of these failings. It is important to note that this model is not intended to capture the detailed temporal processes underlying participants' decisions – this is difficult to do purely from behavior[11]. Instead, the model offers an abstract functional account of what causes answers to be erroneous, namely, a limited processing resource that has to be divided between player types. Examining the different conditions in the task through the medium of the model allows us to parametrize for different participants how player types draw on the resource (briefly: in a precedence hierarchy); how errors creep in when the resource is insufficient for a player type (in terms of both bias and variance); and how the quantity of available resource increases with extra time.

More precisely, we compared multiple potential structural models in terms of how well they fit the answers provided by participants (**Fig. 1g; Supplementary Fig. 2**). The best-fitting model (Model 22, see **Methods**) predicted most participants' answers accurately ($M = 59.8\%$, 95% CI: 57.8 to 61.8; chance $= 9.1\%$), and accounted for 86% of the variance in participants' answers ($R^2 =85.9\%$, 95% CI: 85.7 to 86.1). The model explained the effects of time and complexity on performance, as reflecting a division of total processing resources between player types. Thus, when many player types appeared together, each type was allocated fewer resources. However, more total processing resources were available when extra time was given for deliberation (i.e., in 2s trials). Lower resource allocation to a type meant that the computation of that type's contribution to the total

number of goals was subject to extra bias (towards a default value) and lower precision (i.e., was noisier; **Fig. 1**h). These features of the model were applicable to participants with both high and low sensitivity to time and complexity (**Supplementary Fig. 3**). In addition, model comparison indicated that resources were not divided equally between players, but rather, participants prioritized high-scoring players, and to a lesser degree, more numerous players and those that appeared nearer the center of the screen (**Fig. 1**i,j). This prioritization is consistent with participants' self-reported strategies, as described in a debrief following the experiment (**Supplementary Fig. 4**a).

We next estimated for each participant the model parameters that control how time (2 parameters: λ, λ'), problem complexity (4 parameters: θ, w_2, w_3, w_4), or both (3 parameters: ω, β_{def}, ϵ; see **Methods**) affect resource allocation and the ensuing computations. Only one of these parameters, namely that which controls the precision of computations performed with maximal resource allocation relative to minimal resource allocation (ω; Eq. 15), captured the observed individual variability in sensitivity to time (**Fig. 1**k) and complexity (**Fig. 1**l). A greater effect of resource allocation on precision (i.e., higher ω) results in higher sensitivity to complexity since more resources can be allocated to each player on low complexity compared to high complexity problems. Similarly, higher ω also results in higher sensitivity to time since it enhances the effect of the increased processing resources available in 2s compared to 1s trials. Thus, both types of sensitivity were to some degree manifestations of a common underlying dimension.

In sum, the model indicates that a critical individual difference rested in how the precision of computation changes with resource allocation. However, by design the model is silent as to how computations are temporally organized, and whether this temporal organization is similar for participants that differ in their sensitivity to problem complexity and time constraints. Thus, we next sought additional insight into this aspect of participants' decision processes by decoding the MEG

signals recorded during task performance, and relating these signals to facets of the computation revealed by the model.

To evaluate different hypotheses about how participants' decision processes were temporally structured, we designed three different analysis methods that extracted information from the MEG signals concerning active internal representations of the players and their role in the computations that were captured by the model.

The first method targeted the type of player the participant was contemplating at any given moment. To determine this, prior to informing participants about the aspect of the task concerned with predicting team scores, we presented them with instances of screens they would later see as part of the main task. Such screens contained different numbers of players of different types, and the only task a participant had to solve was simply to count how many players of a given type were depicted (**Supplementary Fig. 5**). We then trained a canonical correlation analysis (CCA[18]) based decoder of MEG signals to predict the number of players the participant counted of the instructed type. Importantly, we verified that decoding was player specific, such that decoded quantities of one player were not positively correlated with actual quantities of another player (one-tailed t-test of the correlation coefficients for each timepoint: $t < 1.5$, df = 39, $p > 0.1$, $r_{pearson} < 0.01$, for all timepoints; **Supplementary Fig. 6**). Thus, we could use this decoder to identify when the players that appeared on a given trial were actively represented, and whether representations of distinct players systematically followed one another in sequence over the course of a trial.

This CCA-decoder was based on averaging across the entire time course of neural response to each type of player in the prior counting task (i.e., averaging across training times in **Supplementary Fig. 5**). Previous studies indicate that responses to such visual stimuli evolve over time in a systematic

8

fashion, with different information encoded at different latencies[9–15]. For instance, the patterns of

activity at 200ms and 400ms following stimulus presentation were shown to be associated with

different degrees of categorical abstraction of the stimuli. Our second analysis examined whether all

of the different temporal components of the neural response were reinstated in the main task, or

whether instead some temporal components were not utilized. To do this, we built decoders specific

to the patterns of activity that characterized each 10ms time bin in the prior task, where only one

player type had to be processed and responses were quick. We then tested the accuracy of each of

these decoders in the main task. This analysis informed us whether participants differed from one

another in the temporal components utilized to represent players.

The first two decoders were based on assessing the number of players of each type. The third

decoder, also built using CCA, attempted to predict the overall number of goals that participants

would ultimately enter. This analysis, which was built using data from the main task (using cross-

validation to avoid over-fitting), showed how a participant's predicted answer evolved over the

course of a trial. However, since participant's answers derived from the players that appeared on the

screen, they would inevitably be partially predictable from a visual representation of the display,

perhaps even before the participant formulated a decision. Therefore, instead of focusing on

whether the MEG signal correctly predicted a participants' answer, we used this decoder to examine

how changes in the predicted answer followed the player representations that were derived using

the first decoder. We expected that the process by which a participant forms an answer would

manifest as a correspondence between the number of goals that a given player scores and how the

predicted answer changes following representation of that player.

A need for greater time to process more information may suggest that different pieces of

information are processed one after the other[2]. However, such inference of serial processing can

rarely be made conclusively based on behavior alone[11], and consequently we used MEG to determine whether high sensitivity to information load and time constraints in our task was coupled to neural evidence for serial processing.

Players composing a team on a given trial could be decoded from cortical activity in both low- and high-sensitivity participants for a period of at least one second after the team appeared on the screen (**Fig. 2**a). To test whether distinct players were represented in sequence during this time, we quantified 'sequenceness', a metric of asymmetry in the cross-correlation function of a given pair of time series, recently shown to detect fast sequences of stimulus representations in MEG[16]. In this case, the time series were the decoded quantities of a pair of player types that appeared together in the trial. Within each pair, types were ordered by the priority the participant accorded them as inferred by the model (see **Fig. 1**), such that positive sequenceness indicated that the lower priority player lagged the higher priority player. We found strong evidence for such player-to-player sequences in high-sensitivity participants (permutation test of sum of t-values across timepoints: $\sum t$ = 212.9, df = 19, p = 0.004, M = 0.0051, extent: 91 timepoints), but no evidence in low-sensitivity participants (permutation test of sum of t-values across timepoints: $\sum t$ = 4.7, df =19, p = 0.76, M = 0.0068, extent: 5 timepoints; **Fig. 2**b,c). Moreover, the average degree of sequenceness throughout the trial was separately correlated with participants' time (p = 0.02, β = 0.38, 95% CI: 0.07 to 0.70) and complexity (p = 0.02, β= 0.39, 95% CI: 0.08 to 0.70) sensitivity, as well as with the common dimension underlying these sensitivities in the model (p < 0.001, β = 0.58, 95% CI: 0.30 to 0.86; robust estimation of regression coefficient for the z-scored measures, tested with random permutations). These results suggest that participants who implemented a serial process, that systematically progressed from high to low priority players, were better able to take advantage of additional available time, but their performance suffered more substantially when facing highly complex problems.

Complexity and time sensitivity reflected a common factor that was captured by the model and associated with MEG evidence supporting sequential processing. However, each type of sensitivity was also characterized by unique inter-individual variance not shared with the other type of sensitivity. To understand what specifically gave rise to differences in complexity sensitivity, we examined the temporal aspect of participants' neural representations during the main task. Since different temporal components of the neural response encode different information[15], it is possible that over- or under-utilization of some components could affect the efficiency of participants' processing. Specifically, we were interested in theoretical accounts that partial encoding of task-relevant information may increase speed at the expense of accuracy[10].

To test this, we used our second decoder to examine how participants adapted their neural response to players in the main task in relation to the prior, counting, task. We found that the early trajectory of the neural response (between 150 and 300 ms) was fairly conserved. Interestingly, some of the later portions of this trajectory were prominent much earlier in time, already appearing simultaneously with the earliest component (i.e., at 150 ms; permutation test of sum of t-values across timepoints: $\sum t$ = 28.0, df = 39, p = 0.01, M = 0.03, extent: 29 components; **Fig. 3**a&b, dashed line), demonstrating a surprising degree of acceleration in the neural response. This was likewise the case for participants with low and high sensitivity to complexity (one-tailed t-test of the difference between groups for each component: t < 1.3, df = 36, p > 0.2, M < 0.03, for all components). However, the two groups differed in the temporal components that they utilized throughout the trial (**Fig. 3**c). While complexity-sensitive participants exhibited early and late components to a similar degree (mean component weighted by decoding accuracy: M = −7 ms, 95% CI: −26 to 18, as compared to uniform utilization), participants with low sensitivity to complexity predominantly exhibited late temporal components (M = +24 ms, 95% CI: 7 to 39; permutation test comparing the

two groups: p = 0.04). Similarly, participants' mean utilized component correlated with how well

they solved the most complex problem when given only 1 s for deliberation (robust estimation of

regression coefficient for the z-scored measures, tested with random permutations: p = 0.02, β =

0.40, 95% CI: 0.08 to 0.71). Thus, a decreased use of early neural representations of task stimuli was

associated with lower sensitivity to complexity.

Perhaps the simplest adaptation one could use to process complex information is to extend the

integration process. Whereas accelerated processing can help cope with complexity under time

pressure, an extended decision process could take fuller advantage of additional available time.

Extended processing may thus result in high sensitivity to time. To test this, we examined whether

participants whose performance was highly sensitive to time represented players for a longer period

within the trial; and whether the player types involved were predominantly those that participants

prioritized in their computations, as indicated by the model.

Players were decodable from the MEG signals in both time-sensitive and time-insensitive

participants immediately after appearing on screen. In time-insensitive participants, these neural

representations lasted only 570 ms after the players disappeared from the screen, even in trials

where 2 sec were available to reach a decision. In contrast, player representation was robustly

evident throughout the entire deliberation epoch in time-sensitive participants **Fig. 4**a). Similarly, we

found that decoding accuracy dropped to zero later in time in time-sensitive (M = 1508 ms following

stimulus offset, 95% CI: 1240 to 1712) compared to time-insensitive (M = 992 ms, 95% CI: 702 to

1312) participants (permutation test comparing the groups: p = 0.01). By comparison, we did not

find a relationship between sustained player representation and participants' sensitivity to

complexity (permutation test comparing the groups: p = 0.72, M = –81 ms, 95% CI: –540 to 370), nor

a relationship between time-sensitivity and player representation on 1 sec trials (**Supplementary Fig.**

7a). Furthermore, players that the model deemed were allocated more processing resources were also more robustly represented in the MEG signal, and this manifestation of participants' allocation of resources was evident during the deliberation period in the time-sensitive group alone (permutation test of sum of t-values across timepoints: $\sum t$ = 332.7, df = 19, p = 0.02, M = 0.02, 95% CI: 0.007 to 0.043; **Fig. 4**b). This latter result confirms the relevance of representations decoded from MEG for understanding participants' decision processes, indicating again that participants who benefitted from additional time processed players for an extended period of time.

Following a similar line of reasoning, we expected time-insensitive participants to have calculated a decision earlier in the trial. To assess this, we used the CCA-based decoder that was trained to predict the total number of goals participants subsequently decided on. We found that participants' decisions could be predicted from the MEG data recorded throughout the trial in both groups of participants (**Supplementary Fig. 7**b). However, such predictions could simply reflect neural representation of the players appearing in the trial, which are themselves predictive of participants' decisions (**Supplementary Fig. 6**e). Evidence for a process of calculation requires the identification of dissociable representations of the quantity of a player and the number of goals the player contributed, with the latter following the former in time.

To test this, we used the same 'sequenceness' metric we previously quantified between players (see **Fig. 2**b,c), but here the two time series were the sum of decoded players, each player multiplied by its scoring ability, and the decoded number of goals the participant was predicted to decide upon (**Fig. 4**c). This analysis identified significant stretches of time during which a change in the decoded quantity of a player was quickly followed by a corresponding shift in the number of goals (**Fig. 4**d,e). This players-to-goals transformation was evident earlier in the trial in time-insensitive participants compared to time-sensitive participants, suggesting that the former indeed employed a shorter

decision process. Interestingly, time-sensitive participants showed both positive and negative players-to-goals sequenceness later in the trial (permutation test of sum of t-values across timepoints: $\sum t$ = 72.1, df = 19, p = 0.008, M = −0.006, extent: 20 timepoints). Negative sequenceness is consistent with a similar transformation but following the *offset* of (i.e., a decrease in) player representations, or alternatively, with a reverse goals-to-players transformation (which may reflect a validatory computation that traces a decision back with a reverse goals-to-players transformation (which may reflect a validatory computation that traces a decision back to the information on which it was based). These results, together with the finding of extended player representations, suggest that time-sensitive participants employed a longer decision process, and were thus able to make use of extra time to solve complex problems more accurately.

The three central temporal features of participants' neural integration processes: sequential player representation (**Fig. 2**b), partial encoding (**Fig. 3**c) and early computation (**Fig. 4**d) were associated with individual variability in sensitivity to time and complexity, and in the modeled sensitivity to resource allocation that underlies them. To examine whether the MEG features were each associated with an independent impact on task performance, we quantified each feature by integrating it over all relevant time points in the trial. Quantified thus, the three features were not correlated with one another across participants (Robust estimation of regression coefficient, tested with random permutations: p > 0.25, β < 0.20, for all pairs). More importantly, we found that each MEG feature was only associated with a single type of sensitivity, when controlling for the other types of sensitivity in a multiple regression model (**Supplementary Fig. 8**). Thus, early goal computation was uniquely associated with low time sensitivity, reduced reinstatement of early temporal components was uniquely associated with low complexity sensitivity, and sequential player representation was uniquely associated with the common underlying sensitivity to resource allocation.

When solving demanding tasks, the human brain has limited processing resources at its disposal, and so typically trades off between different aspects of task performance[19–21]. In examining how people integrate multiple simultaneously available elements of information, we found substantial variation in how well participants processed complex problems, and conversely, how much advantage they gained from an allowance of extra time to do so. To uncover associated variations in participants' underlying neural dynamics, we used a model-based analysis of MEG signals that uncovered a rapid evolution of cortical representations for distinct elements of the experimental task. This analysis revealed a multiplicity of information integration processes differing in temporal structure. In particular, we extracted three structural factors, each revealing a different way a participant could cope with a complex problem involving a diverse set of elements.

The factor associated with both time and complexity sensitivity identified decision processes that involved sequences of elements in an order that reflected the relative importance participants accorded to those elements. Decision processes involving such sequences led to better solutions for problems posing low-to-moderate processing demands, whereas decision processes without detectable sequences were associated with better solutions for problems posing high processing demands. Our computational model was able to infer the existence of this central dimension of individual difference from participants' choice behavior. However, decoding cortical activity was necessary to understand the aspect of participants' integration processes that gave rise to these differences among participants, revealing deployment of a systematic sequential process.

Equally important, decoding participants' neural activity revealed two additional factors, which computational modeling based on behavior alone could not uncover. One factor was unique to complexity sensitivity, and concerned the nature of the representations that supported participants'

15

computations. Participants who were not sensitive to complexity only reinstated late temporal components of the neural response (> 250 ms), indicating that partial encoding in this manner could underlie improved efficiency. A second factor was unique to time sensitivity, and concerned a prolonged integration process. The latter was specifically apparent in 2s trials, with the elements of the problem being decodable between 1s and 2s in time sensitive participants alone, and indeed favoring those elements that were more accurately reflected in participants' answers. Similarly, evidence of computation of one's answer was evident earlier in the trial in time-insensitive participants.

Unfortunately, we lacked sufficient numbers of participants to examine interactions among the three factors. Thus, for instance, there was no evidence that the player-to-player sequentiality of the combined factor also lasted into the additional second of processing performed by temporally-sensitive participants. Equally, whether player-to-player sequenceness is equally likely when player representations are only partially reinstated is unclear. These facets, completely unexpected from a purely behavioral analysis, are pressing targets for future work that avail of tasks that can dissociate between these structurally distinct processes.

Our main result, concerning sequential element representation, resonates with a familiar dichotomy in computer science, psychology and neuroscience literatures between parallel and serial processing. In these literatures, parallel processing is proposed as a means for coping with large quantities of information quickly[1–3], but when implemented in the brain is suggested to compromise precision[4]. By contrast, performing operations serially, one after the other, allows an agent to devote as much resource as necessary to each operation separately, enabling more precise execution. However, this strategy may fail if the allowed time is insufficient to complete all required operations. Our finding of sequences of player representations specifically in those participants who

demonstrated higher precision on simple problems, but greater sensitivity to complexity, indicates

that the parallel/serial distinction is important for an understanding of how people integrate

information. Serial processing of elements that compose a single task has previously been examined

in humans only by analysis of choice and eye gaze data[22,23], though neural recordings have recently

provided evidence for such processing in macaques[24]. Our MEG method provides a means to study

such serial processes with human neural measurements that avoids pitfalls that often plague

behavioral studies of serial and parallel processes[25].

It is probable that the processes implemented in our task reflect, to some degree, an individual's

preferred processing style[26–32]. Inference of differences in processing style, rather than in overall

ability, accords with an absence of corresponding differences in independently measured cognitive

abilities, including working memory capacity and fluid intelligence. These latter quantities solely

predicted better *overall* performance in the task (**Supplementary Fig. 4**b), whereas our results reveal

that different people are better at different type of problems. Future work might usefully investigate

how information integration styles relate to risk of psychiatric disorders that involve primary

disturbances in cognitive and attentional processes[33,34], such as schizophrenia, autism and attention-

deficit disorder.

Methods

Participants

40 human participants, aged 19–34 years, 25 female, were recruited from a participant pool at

University College London. Exclusion criteria included age (younger than 18 or older than 35),

neurological or psychiatric illness, and psychoactive drug use. No statistical methods were used to

pre-determine sample sizes but, to allow sufficient statistical power for comparisons between two

groups of participants, we set the sample size to roughly double the sample size used in recent

magnetoencephalography (MEG) studies on dynamics of neural representations[15,17], and to align

with recent neuroimaging studies of individual differences in cognitive function[32,35,36]. Participants

received monetary compensation for their time (£40) in addition to a small bonus (between £5 and

£9) that depended on how well they performed the task. The experimental protocol was approved

by University College London's (UCL) local research ethics committee, and informed consent was

obtained from all participants.

Task

To test integration of diverse information into coherent decisions, we designed a decision making

task in which participants had to determine how many goals different sets of players would score

(**Fig. 1**b). Players could be of 4 different types, each scoring a different number of goals per game

(1.6, 1.2, 0.6, and minus 0.4). The correct decision was simply the sum of goals scored by each set of

players, rounded to the closest natural number. Thus, players of different types differed in how likely

they were to impact the correct decision. We set players' scoring abilities to non-integer numbers so

that participants would not be able to compute the sum of goals precisely for complex sets of

players, and we included one player type that subtracts goals (minus 0.4) to dissuade participants

from ignoring player type and simply relying on the total number of players.

To ensure that participants knew well how many goals each player type scores, participants first

trained on each player type separately until reaching a performance criterion (**Supplementary Fig.**

1). Then, training continued to teams consisting of two types of players, and finally to teams with 3

types of players. In each trial, the number of players of each type was always between 1 and 3, and

all player types were equally likely to appear in any number, alone or matched with any of the other

players. Players were assigned random positions on the screen, ensuring that they do not overlap

yet are closest as possible to the center of the screen. Feedback was provided following each

decision, indicating the correct number of goals and whether decisions were 'correct', 'incorrect' or 'very close' (within 1 of the correct number). Following every 10 trials or 3 consecutive 'incorrect' decisions, participants were reminded of the number of goals each player type scores. Participants then performed the main task, in which feedback and reminders were no longer provided. The task was divided into 7 blocks of trials, 48 randomly ordered trials each.

To test the impact of problem complexity on participant performance, we manipulated the number of player types appearing together in a trial. Thus, the task included an equal number of trials with 1, 2, 3, and 4 player types. The experiment included all possible team configurations so as to minimize the number of times each configuration repeated. To test how time constraint impacts performance, we gave participants 2 s to reach a decision in blocks 1, 3, 5 and 7, but only 1 s in blocks 2, 4, and 6. When the time for decision ended, a bar indicating zero goals appeared on the screen, and participants were given just enough time (1 s + 250 ms per goal) to comfortably adjust the bar to the correct number of goals (one button press moved the bar one goal). The decision was recorded as the number of goals the bar pointed to when time expired. Participants' button presses were analyzed to ensure that they did not exploit the changing response interval to derive the correct answer (**Supplementary Fig. 9**). Participants were notified before each block how much time will be available, but they did not know in advance how many player types each trial will involve, and thus, there was limited scope for adjusting processing strategy during the experiment. Finally, to test the impact of arousal and motivation on performance, we notified participants before ⅙ of trials that the next trial will have a larger (×10) effect on the monetary bonus they receive. The results of the latter manipulation are beyond the scope of this paper and will be reported elsewhere. Complementary analyses verified that none of the present study's main findings were specifically attributable to the high-stake trials. We note that performance was slightly better on these trials (Bootstrap test: p = 0.02, M = +2.5%, 95% CI: 0.4 to 4.8), and such trials did not show the otherwise evident relationship between time-sensitivity and early player-to-goal sequenceness.

Measures of sensitivity

Since participants might be able to provide approximate, but not precise, answers by simply relying on general features of the problem (e.g., the total number of players), we focused our model-free analyses on whether participants provided precisely correct answers. This was later complemented by model-based analysis that considered how close participants were to the correct answer and disentangled the different types of computations this reflected (see next subsection). To quantify the degree to which participants were affected by constraints (i.e., 'Sensitivity to time'), we computed participants' accuracy (proportion of precisely correct decisions) in 2s trials minus accuracy in 1s trials. To quantify how participants were affected by problem complexity when little time was available, we computed their accuracy on 1s trials with 1 player type minus accuracy on 1s trials with 4 player types. We also combined both measures, after z scoring, using principal component analysis (PCA). The first component, which weighted time and complexity sensitivity equally (coefficients = [0.71, 0.71], variance = 1.48), was used as a general measure of sensitivity. Alternative measures of these three types of sensitivities (time, complexity, and combined) were derived from PCA of participants accuracy levels in the 8 different trials types (**Supplementary Table 1**). Complementary analyses showed that these PCA-derived measures related to the reported MEG indices (from **Fig. 6**) in the same way as the accuracy-differences measures.

Decision making model: rounding

To gain insight into participants' decision processes we compared multiple models in terms of how well they explained participants' decisions in the task. Model comparison proceeded in stages, where in each stage we tested a different aspect of participants' processing. More complex models were penalized by means of the Bayesian Information Criterion[37] (BIC).

We first tested whether participants rounded scores before (Model 1) or after (Model 2) summing them up.

Model 1 ('Precise scoring'; Eqs. 1,2) simply multiplies the number of players of each type with that type's scoring coefficient:

$$p(\text{goals}|\boldsymbol{s}) = \mathcal{N}(\boldsymbol{\beta}^{\mathrm{T}}\boldsymbol{s}, \sigma^2 \textstyle\sum \boldsymbol{s}), \tag{1}$$

where $\boldsymbol{s} = [s_1 \quad s_2 \quad s_3 \quad s_4]^{\mathrm{T}}$ is the number of players of each type, $\boldsymbol{\beta} = [\beta_1 \quad \beta_2 \quad \beta_3 \quad \beta_4]^{\mathrm{T}}$

contains the scoring coefficients, and σ^2 is a variance parameter that is scaled by the number of

players. A decision is sampled from this posterior distribution (Eq. 1) and rounded to the nearest

whole number. Thus, the likelihood of a particular decision being observed is computed as follows:

$$p(\text{decision}|\boldsymbol{s}) = \int_{\text{decision}-\frac{1}{2}}^{\text{decision}+\frac{1}{2}} p(\text{goals}|\boldsymbol{s}), \tag{2}$$

where in the special boundary cases of $\text{decision} = 0$ and $\text{decision} = 10$, the integral's interval

starts from $-\infty$ or ends at ∞, respectively.

Model 2 ('Rounded scoring'; Eqs. 1,2) performs the same computation, but it rounds the scores of

each type of player to the nearest integer before summing over player types.

Model 3 ('Mixed precise and rounded'; Eqs. 1–3) reflects a compromise between the first two

models in that its scoring coefficients are a linear combination of the two sets of coefficients:

$$\boldsymbol{\beta} = \boldsymbol{\alpha}\boldsymbol{\beta}_{\mathrm{M1}} + (1 - \boldsymbol{\alpha})\boldsymbol{\beta}_{\mathrm{M2}}, \tag{3}$$

where $\boldsymbol{\beta}_{\mathrm{M1}}$ and $\boldsymbol{\beta}_{\mathrm{M2}}$ are the coefficients from Model 1 and Model 2, respectively, and $\boldsymbol{\alpha}$ is a vector

of mixing coefficients. Model 3 fit best.

Decision making model: incomplete processing

We next tested whether participants took into account all players. To this end, we compared the

best-fitting model from the previous step (Model 3) to variants of this model that ignore a certain

proportion (Model 4) or number (Model 5) of players, or account for some players by means of a

default value that does not reflect player type (Model 6).

Model 4 ('Proportional loss'; Eqs. 2–5) misses a fixed proportion of all players:

$$s_i' = s_i - \gamma s_i, \tag{4}$$

where γ is the loss proportion and i indicates player type, and the decision is computed with respect to this lossy transformation of s:

$$\mathrm{p}(\text{goals}|s) = \mathcal{N}(\boldsymbol{\beta}^{\mathrm{T}}s', \sigma^2 \Sigma s). \tag{5}$$

Model 5 ('Thresholded loss'; Eqs. 2,3,5,6) computes the decision similarly to Model 4 but only misses a fixed proportion above a certain number of players:

$$s_i' = s_i - \gamma \frac{s_i}{\Sigma s} \max[\Sigma s - \epsilon, \ 0], \tag{6}$$

where ϵ is the threshold above which players are missed.

Model 6 ('Regression to a default'; Eqs. 2,3,7,8) applies the threshold ϵ similarly to Model 5, but instead of ignoring players, it accounts for them via a default scoring coefficient (β_{def}):

$$s_i' = s_i \left(1 - \frac{\max[\Sigma s - \epsilon, \ 0]}{\Sigma s} \right), \tag{7}$$

$$\mathrm{p}(\text{goals}|s) = \mathcal{N}(\boldsymbol{\beta}^{\mathrm{T}}s' + \beta_{\mathrm{def}}\Sigma(s - s'), \sigma^2 \Sigma s). \tag{8}$$

Decision making model: division of recourses

We next tested whether participants' decisions are better explained by assuming that processing resources had to be divided between players that appeared together. To this end, we compared the best-fitting model from the previous stage (Model 6) to variants of this model in which resources are divided between players, determining how precisely they are computed (Model 7), how likely they are to be discriminated (Model 8), or both (Model 9).

Model 7 ('Divided resources – variance; Eqs. 2,3,7,9–15) computes more precisely the contribution of players that are allocated more resources. The model equally divides its resources (r) between the player types that appear together in the trial:

$$r_i = \frac{1}{\theta \|s\|_0}, \tag{9}$$

22

where $\|\boldsymbol{s}\|_0$ is the number of player types, and θ is a scaling factor that accounts for differences among participants in the total amount of allocated processing resources (i.e., lower θ indicates greater resource allocation). Optimal processing ($o_i = 1$) of player type i is achieved only if resources allocated to that type exceed a value of 1:

$$o_i = \min[r_i, \ 1]. \tag{10}$$

Thus, players are divided into optimally processed ($\boldsymbol{s}_+$) and minimally processed ($\boldsymbol{s}_-$) components:

$$\boldsymbol{s}_+ = \boldsymbol{o} \circ \boldsymbol{s}, \tag{11}$$

$$\boldsymbol{s}_- = (1 - \boldsymbol{o}) \circ \boldsymbol{s}, \tag{12}$$

and the optimally processed component increases decision variance less:

$$p(\text{goals}|\boldsymbol{s}) = \mathcal{N}\big(\boldsymbol{\beta}^{\mathrm{T}}\boldsymbol{s}' + \beta_{\text{def}}\Sigma(\boldsymbol{s} - \boldsymbol{s}'), \sigma_+^2 + \sigma_-^2\big), \tag{13}$$

where

$$\sigma_-^2 = \sigma^2 \Sigma \boldsymbol{s}_-, \tag{14}$$

$$\sigma_+^2 = \frac{\sigma^2}{\omega} \Sigma \boldsymbol{s}_+, \tag{15}$$

and ω defines the precision of the computation with maximal relative to minimal resource allocation.

Model 8 ('Divided resources – default; Eqs. 2,3,9–12,16,17) divides processing resources similarly to Model 7, but this division only determines which players are partially accounted for by a default value:

$$s_i' = s_{+i} + s_{-i}\left(1 - \frac{\max[\Sigma\boldsymbol{s}_- - \epsilon, \ 0]}{\Sigma\boldsymbol{s}_-}\right), \tag{16}$$

while precision is equal for the minimally and maximally processed components:

$$p(\text{goals}|\boldsymbol{s}) = \mathcal{N}\big(\boldsymbol{\beta}^{\mathrm{T}}\boldsymbol{s}' + \beta_{\text{def}}\Sigma(\boldsymbol{s} - \boldsymbol{s}'), \sigma^2 \Sigma\boldsymbol{s}\big), \tag{17}$$

Model 9 ('Divided resources – variance & default'; Eqs. 2,3,9–16) combines both effects of resource allocation implemented in Models 7 and 8. This model fitted best.

Decision making model: player prioritization

We next tested whether participants' tended to prioritize some players over others. To this end, we compared between the best-fitting model from the previous stage (Model 10) and variants of this model that allocate more resources to players that score more goals (Model 11), to players of which type there are more (Model 12), and to players that appear nearer the center of the screen (Model 13).

Model 10 ('Highest scoring'; Eqs. 2,3,10–16,18) ranks the player types that appear in the trial by the number of goals they score. Player types that do not appear in the trial are assigned a weight of 0, the highest ranked players are assigned the weight $w_1 = 1$, and all other players are assigned the weights $w_j = \rho_j w_{j-1}$, where j is player rank, and $[\rho_2 \ \rho_3 \ \rho_4]$ are free parameters in the range of 0 to 1. Resources are then divided in accordance with the weights:

$$r_j = \frac{w_j}{\sum \boldsymbol{w}}. \tag{18}$$

Since the player that subtracts goals is unique we surmised that participants could vary in how much resources they allocated it, and thus, we included in Model 10 a free parameter (υ) that allowed this player to be ranked anywhere among the three other players. Model comparison favored the addition of this latter parameter (BIC difference = 8).

Model 11 ('Most numerous'; Eqs. 2,3,10–16,18) uses a similar computation to divide resources but ranks player types by how many players of each appear in the trial, whereas Model 12 ('Most central'; Eqs. 2,3,10–16,18) ranks player types by how close to the center of the screen each is displayed (based on the shortest distance for any player of each type).

In addition, we also tested whether combinations of the above rankings methods could explain participants' decisions better than each ranking alone. To this end, we constructed models which combine multiple types of rankings by means of a weighted average:

$$\boldsymbol{w} = \sum_m \phi_m \boldsymbol{w}_m, \tag{19}$$

where $\boldsymbol{w}_m$ is the weights assigned by Model m, and ϕ_m are non-negative mixing coefficients that sum to 1. Models 13 to 16 cover all possible combinations of Models 10 to 12 (Eqs. 2,3,10–16,18,19).

Decision making model: effect of time

Finally, we tested what variation in the process that participants implemented best explained differences in performance between 1 s and 2 s trials. To this end, we compared between the best-fitting model from the previous stage (a combination of Models 10–12) and variants of this model that allowed the default scoring coefficient (Model 17), the player quantity threshold for regression to the default (Model 18), the decision variance with minimum (Model 19) and maximum (Model 20) resource allocation, and processing resources capacity (Model 21) to vary between 1 s and 2 s trials.

In Model 17 ('Default score'), the default scoring coefficient in 2 s trials is a multiple of the default scoring coefficient in 1 s trials (i.e., $\beta_{\mathrm{def\_2s}} = \lambda \beta_{\mathrm{def\_1s}}$, where $\lambda \geq 0$). In Model 18 ('Default score threshold'), the number of players beyond which players are accounted for by means for the default scoring coefficient in 2 s trials is a multiple of the same threshold in 1 s trials (i.e., $\epsilon_{2s} = \lambda \epsilon_{1s}$). In Model 19 ('Decision variance with minimum resources'), the variance associated with the minimum resources component in 2 s trials is a multiple of the same variance in 1 s trials (i.e., $\sigma^2_{+2s} = \lambda \sigma^2_{+1s}$). In Model 20 ('Decision variance with maximum resources'), a similar multiplication applies to the variance associated with the maximum resources component (i.e., $\sigma^2_{-2s} = \lambda \sigma^2_{-1s}$). In Model 21 ('Processing capacity'), the parameter that scales the total amount of resources in 2 s trials is a multiple of the same parameter in 1 s trials (i.e., $\theta_{2s} = \lambda \theta_{1s}$).

Finally, since model comparison provided considerable support for the last two factors (from Models 20 and 21), we tested a model that incorporates both (Model 22). Model 22 fitted participants' answers the best, and thus we provide pseudocode describing its operations for a single trial.

MODEL 22 (21 free parameters)

$s \leftarrow$ quantity of players of each type, excluding absent types, ordered from high to low scoring

STEP 1: allocate resources

Truncate w so that its length is the same as s

$w_{\text{type}} \leftarrow w$ ordered according to player scoring ability (high to low, negative scorer position

determined by free parameter)

$w_{\text{quantity}} \leftarrow w$ ordered according to player quantity (high to low)

$w_{\text{location}} \leftarrow w$ ordered according to player distance from center of screen (low to high)

$w_{\text{total}} \leftarrow \phi_{\text{type}} w_{\text{type}} + \phi_{\text{number}} w_{\text{number}} + \phi_{\text{location}} w_{\text{location}}$

IF this is a 1 sec trial THEN $r \leftarrow \dfrac{w_{\text{total}}}{\theta \sum w_{\text{total}}}$ ELSE $r \leftarrow \dfrac{w_{\text{total}}}{\lambda \theta \sum w_{\text{total}}}$

STEP 2: divide players into optimally and minimally processed components

FOR $i = 1$ to number of player types DO

    IF $r_i > 1$ THEN $o_i \leftarrow 1$ ELSE $o_i \leftarrow r_i$

$s_+ \leftarrow o \circ s$

$s_- \leftarrow (1 - o) \circ s$

STEP 3: divide players into differentiated and undifferentiated components

IF $\sum s_- < \epsilon$ THEN $d \leftarrow 1$ ELSE $d \leftarrow \dfrac{\epsilon}{\sum s_-}$

$s' \leftarrow s_+ + d \cdot s_-$

$s'' \leftarrow s - s'$

STEP 4: compute mean of predicted answer

$$\boldsymbol{\beta}_{\text{round}} \leftarrow \text{ROUND}(\boldsymbol{\beta} \circ \boldsymbol{s}) \circ \frac{1}{\boldsymbol{s}}$$

$$\text{mean} \leftarrow \boldsymbol{\alpha}^{\text{T}}(\boldsymbol{\beta} \circ \boldsymbol{s}') + (1 - \boldsymbol{\alpha})^{\text{T}}(\boldsymbol{\beta}_{\text{round}} \circ \boldsymbol{s}') + \beta_{def} s''$$

STEP 5: compute variance of predicted answer

$$\sigma_+^2 = \frac{\sigma^2}{\omega} \textstyle\sum \boldsymbol{s}_+$$

IF this is a 1 sec trial THEN $\sigma_-^2 = \sigma^2 \sum \boldsymbol{s}_-$ ELSE $\sigma_-^2 = \lambda' \sigma^2 \sum \boldsymbol{s}_-$

$$\text{variance} \leftarrow \sigma_+^2 + \sigma_-^2$$

STEP 6: compute likelihood given actual answer

IF goals > 0

THEN $\text{p(goals}|\boldsymbol{s}) \leftarrow \int_{\text{goals}-\frac{1}{2}}^{\text{goals}+\frac{1}{2}} \mathcal{N}(x|\text{mean, variance})\, dx$

ELSE $\text{p(goals}|\boldsymbol{s}) \leftarrow \int_{-\infty}^{\frac{1}{2}} \mathcal{N}(x|\text{mean, variance})\, dx$

Model fitting

To fit the parameters of the different models to participants' decisions, we used a hierarchical expectation-maximization procedure[38]. We first sampled 10^4 random parameterizations from predefined group-level prior distributions. Then, we computed the likelihood of observing participants' choices given each parametrization, and used the computed likelihoods as importance weights to resample (and fit the parameters of) the group-level prior distributions. These steps were repeated iteratively, with gradually increasing numbers of samples (starting with 10^4 samples, and increasing by a factor $10^{0.5}$ every two iterations), until stable estimates were obtained. Finally, to derive the best-fitting parameters for each individual participant, we computed a weighted mean of the final batch of parametrizations, in which each parameterization was weighted by the likelihood it assigned to the individual participant's decisions. Player coefficients ($\boldsymbol{\beta}, \beta_{\text{def}}$) were modeled with normal distributions (initialized with $\mu = 0$ and $\sigma = 1$), fractional parameters ($\boldsymbol{\alpha}, \boldsymbol{\rho}, \boldsymbol{\phi}$) were modeled with Beta (initialized with $\alpha = 1$, $\beta = 1$) or Dirichlet distributions (initialized with all $\alpha = 1$) as

appropriate, and all other parameters were modeled with Gamma distributions (initialized with k = 1, θ = 1). Modeling was performed in Matlab (MathWorks). See **Supplementary Software** for relevant code.

Model comparison

To compare pairs of models, in terms of how well each model accounted for participants' choices, we estimated the log Bayes factor[39] by means of an integrated Bayesian Information Criterion (iBIC[36, 40]). We estimated the evidence in favor of each model ($\mathcal{L}$) as the mean likelihood of the model given 10^7 random parameterizations drawn from the fitted group-level priors (in the final model comparison, $10^{7.5}$ random parameterizations were required to obtain stable estimates of $\mathcal{L}$). We then computed the iBIC by penalizing the model evidence to account for model complexity as follows: $\text{iBIC} = -2 \ln \mathcal{L} + k \ln n$, where k is the number of fitted parameters and n is the number of participant decisions used to compute the likelihood. Lower iBIC values indicate a more parsimonious model fit. We validated our model comparison procedure by generating simulated datasets using each model, and applying our procedure to recover the model that generated each dataset (**Supplementary Fig. 10**).

Resource allocation

We used the model to infer the amount of processing resources each participant allocated to each player type on each trial. To this end, we sampled 1,000 random parameterizations from the posterior probability fitted to each participant, and we computed the resource allocation that each parameterization of the model yielded in each individual trial. Then, for each trial, we computed a weighted mean of the 1,000 resource allocation vectors, where the weight of each vector was determined by the likelihood it assigned to the participant's decision on that trial.

MEG acquisition

MEG was recorded continuously at 600 samples/second using a whole-head 275-channel axial gradiometer system (CTF Omega, VSM MedTech, Canada), while participants sat upright inside the

scanner. A projector displayed the task on a screen ~80 cm in front of the participant. Participants made responses by pressing a button box using the fingers they found most comfortable. Pupil size and eye gaze were recorded at 250 Hz using a desktop-mounted EyeLink II eyetracker (SR Research).

MEG preprocessing

Preprocessing was performed using SPM12 (Wellcome Trust Centre for Neuroimaging, University College London) and the Fieldtrip toolbox[41] in MATLAB (MathWorks). Data from two sensors were not recorded due to a high level of noise detected in routine testing. Data were first inspected visually and 3 jump artifacts were removed manually. Then, independent component analysis was used to remove components that corresponded to eye blinks, eye movement and heart beats. Based on previous experience[15,16], we expected stimuli to be represented in low frequency fluctuations of the MEG signal. Therefore, to remove fast muscle artifacts and slow movement artifacts, we band-pass filtered the data between 0.1 and 20 Hz using a third-order Butterworth IIR filter. Acausal symmetric filtering was used to avoid introducing asymmetricities into the data that could bias the sequenceness analyses. Thus, stimulus responses could appear slightly before onset of a stimulus. Finally, the data were resampled from 600 Hz to 100 Hz to conserve processing time and improve signal to noise ratio. Therefore, data samples used for analysis were length 273 vectors spaced every 10 ms.

Pre-task stimulus exposure

To allow decoding from MEG of the identity and quantity of players that participants were processing, we first instructed participants to count players of each type in turn (**Supplementary Fig. 5**a). On each trial, the target player type was indicated textually, and then players appeared on the screen in teams similar to those used in the main task. Participants responded by pressing one of three buttons ("one", "two" or "three"), continuing until they made at least 30 correct responses for each player type. To ensure robust decoding from MEG, we had players of different types differ in color, shape, texture and semantic category[9–14] (**Fig. 1**a). 6 types were used at this stage: face, frog,

tomato, roundabout sign, hand, and desert, and 4 of these were randomly picked to serve as players in the main task. Importantly, participants did not yet know what the main task will be or that the figures represent players that score goals, ensuring that no information about goals could be represented in the MEG data at this stage.

MEG decoding: players

To train the decoder we labeled each MEG sample from the stimulus exposure stage with a vector comprising four dimensions, one for each player type. In each trial, the target player type was labeled with its counted quantity, and all other player types were labeled with zero. We then derived the relationship between the quantities and the MEG data using regularized linear canonical correlation analysis (CCA[42]). Regularized CCA is particularly useful for decoding players in this task since it prioritizes MEG features that provide information about multiple player types. This analysis was performed separately for each time bin between 400 ms before and 600 ms after players appeared on the screen resulting in 101 decoders (the target player was indicated textually 250 ms before players onset, and median response time was 666 ±14 ms after players onset). We tested each decoder on each of the 101 time bins in a separate set of trials, using 5-fold cross validation. Decoding performance was computed as the correlation between actual and decoded player quantities, averaged across player types (**Supplementary Fig. 5**b; **Supplementary Fig. 6**). Decoder training and testing were performed with each of 5 settings of the CCA regularization parameter (0.5, 5, 50, 500, 5000). A setting of 50 yielded the best cross-validated decoding performance and was thus used for all ensuing analyses.

Decoding performance started to increase 150 ms following players onset, and thus, we used decoders trained on all time bins following the 150 ms mark to decode player representations in the main task (46 decoders). For each time bin in the main task, decoded quantities were averaged across decoders, z scored across trials, and baseline corrected based on the 200 ms period preceding trial onset. Decoding performance was computed separately for trials with 1, 2, 3 and 4 player types.

Since the MEG data and the decoded quantities featured pronounced alpha oscillations, decoded time series were smoothed with a 250 ms sliding average for analyses concerned with persistence of representation (**Figs. 3**a;**5**a,b).

MEG decoding: answers

To decode from MEG the number of goals a participant was about to decide on, we trained CCA decoders on the relationship between participants' answers and MEG recorded during the main task. Decoders were trained on and applied to separate subsets of trials, using 5-fold cross validation. The analysis was performed separately for each time bin of 1 s and 2 s trials.

Sequenceness measure

To investigate how different representations related to one another in time, we used a recently developed measure for detection of sequences of representations in MEG[16], inspired by related work on spiking dynamics in rodents[43]. 'Sequenceness' is computed as the difference between the cross-correlation of two (or more) time series with positive and negative time lags. Since it focuses on asymmetries in the cross correlation function, this measure is useful for detecting sequential relationships even between closely correlated (or anti-correlated) time series. Due to the presence of alpha oscillations in our data, and the possibility that such oscillations may reflect temporal quanta of information processing[44], we tested for sequenceness with time lags of up to 200 ms, which is sufficient for capturing the relationship between successive alpha cycles. Cross correlations were computed over 200 ms sliding windows, and were normalized such that autocorrelations at time lag zero equals one. The difference between cross correlations with positive and negative time lags indicated whether changes in one time series tended to be followed by similar changes in the other time series. We validated the sequenceness analysis by testing it on randomly generated correlated time-series (**Supplementary Fig. 11**). See **Supplementary Software** for relevant code.

Players-to-goals sequences

To determine how participants' answers evolved in MEG in relation to player representations we computed the sequenceness between a decoded answer and a weighted sum of decoded players, where each player is weighted by the number of goals it scores. Positive sequenceness indicates that an increase in the representation of a player was followed by an increase in the number of goals a participant was likely to decide on that is proportional to the player scoring ability.

Player-to-player sequences

To determine whether players were represented in MEG one after the other, we first defined an ordering of players for each participant, based on the prioritization employed by the decision making model that best-fitted the participant's decisions. We then separately computed the sequenceness between the decoded time series of each pair of players, with players ordered such that positive sequenceness indicated a transition from the high priority to the low priority player. Finally, we averaged the computed sequenceness measures across the different pairs.

Time series analyses

To control for multiple comparisons, we tested for statistical significance within time series by means of a permutation test[45]. Specifically, we conducted a separate t test for each time point, and computed the sum of t values over each stretch of consecutive time points where t values exceeded 1.7 (corresponding to a one-tailed p value of 0.05). The data was then shuffled 10,000 times as described below, and the same procedure was carried out to find the maximum sum-of-t-values in each shuffled data set. Finally, a two-tailed p value for each stretch in the original unshuffled time series was computed as the proportion of shuffles that yielded a larger maximum sum-of-t, compared to the sum-of-t in the original stretch. When testing differences between two time series that represented two groups of participants, shuffling was achieved by randomly reassigning participants to groups. When testing a single time series for difference from zero, shuffling was achieved by multiplying each time series by minus one with a 0.5 probability (either the whole time series was multiplied or none of it was). All time series were smoothed with a 100 ms moving

average unless otherwise noted. We validated this method by testing it on random time-series generated by a zero-mean Gaussian process (**Supplementary Fig. 12**).

Other statistical tests

To mitigate the impact of potential outliers, all linear relationships between two variables were tested using robust regression on the z-scored variables with default MATLAB options (bisquare weighting, tuning constant 4.685). Two-tailed p values were computed using a permutation test with 10,000 random permutations. Where more than one relationship was tested, p values that account for multiple comparisons were computed as the proportion of permutations for which the maximum regression coefficient across relationships was greater than the original regression coefficient. All reported statistical tests are two-tailed.

Post-experiment questionnaires

Following the experiment, participants filled out a standard debriefing questionnaire in which they reported how they computed the number of goals each team would score (**Supplementary Fig. 4**a). In addition, to assess dimensions of individual differences that could affect task performance, we had participants perform the Corsi block-tapping task[46] (excluding one participant due to a technical issue) and the matrix reasoning component of the Wechsler abbreviated scale of intelligence[47]. In addition, we had participants fill out the analysis-holism scale[30], the abridged autism-spectrum quotient[48], and the World Health Organization adult attention-deficit/hyperactivity disorder self-report scale[49].

Data availability

The data that support the findings of this study are available from the authors on reasonable request.

Code availability

Custom scripts used for this study are provided as **Supplementary Software**, and available at

https://github.com/eeldar/football-task (sequenceness analysis and computational model) and at

https://github.com/eeldar/model-fitting (model fitting and model comparison).

Competing Interests statement

The authors declare no competing interests.

Author Contributions

Conceptualization, E.E.; Methodology, E.E., G.B., Z.K. and P.D.; Investigation, E.E., and G.B.; Writing –

Original Draft, E.E.; Writing – Review & Editing, E.E., Z.K., P.D. and R.J.D.; Funding Acquisition, R.J.D.;

Supervision, P.D., and R.J.D.

Acknowledgements

References

1. Rumelhart, D. E. & McClelland, J. L. (Eds.) *Parallel Distributed Processing: Explorations in the Microstructure of Cognition*. (Cambridge, MA, MIT Press, 1986)

2. Treisman, A. M. Strategies and models of selective attention. *Psychol. Rev.* **76**, 282 (1969)

3. Bergen, J. R. & Julesz, B. Parallel versus serial processing in rapid pattern discrimination. *Nature* **303**, 696–698 (1983)

4. Feng, S. F., Schwemmer, M., Gershman, S. J. & Cohen, J. D. Multitasking versus multiplexing: Toward a normative account of limitations in the simultaneous execution of control-demanding behaviors. *Cogn. Affect. Behav. Neurosci.* **14**, 129–146 (2014)

5. Gold, J. I. & Shadlen, M. N. The neural basis of decision making. *Annu. Rev. Neurosci.* **30**, 535–574 (2007).

6. Heitz, R. P. & Schall, J. D. Neural mechanisms of speed-accuracy tradeoff. *Neuron* **76**, 616–628 (2012)

7. Hanks, T., Kiani, R. & Shadlen, M. N. A neural mechanism of speed-accuracy tradeoff in macaque area LIP. *Elife* **3**, e02260 (2014)

8. Hawkins, G. E., Forstmann, B. U., Wagenmakers, E. J., Ratcliff, R. & Brown, S. D. Revisiting the evidence for collapsing boundaries and urgency signals in perceptual decision-making. *J. Neurosci.* **35**, 2476–2484 (2015)

9. Marti, S., King, J. R. & Dehaene, S. Time-resolved decoding of two processing chains during dual-task interference. *Neuron* **88**, 1297–1307 (2015)

10. Chalk, M., Marre, O. & Tkačik, G. Toward a unified theory of efficient, predictive, and sparse coding. *Proc. Natl. Acad. Sci. USA* **115**, 186–191 (2018)

11. Williams, P., Eidels, A. & Townsend, J. T. The resurrection of Tweedledum and Tweedledee: Bimodality cannot distinguish serial and parallel processes. *Psychon. Bull. Rev.* **21**, 1165–1173 (2014)

12. Carlson, T., Tovar, D. A., Alink, A. & Kriegeskorte, N. Representational dynamics of object vision: the first 1000 ms. *J. vis.* **13**, 1 (2013)

13. Isik, L., Meyers, E. M., Leibo, J. Z. & Poggio, T. The dynamics of invariant object recognition in the human visual system. *J. Neurophysiol.* **111**, 91–102 (2014)

14. Cichy, R. M., Pantazis, D. & Oliva, A. Resolving human object recognition in space and time. *Nat. Neurosci.* **17**, 455–462 (2014).

15. Kurth-Nelson, Z., Barnes, G., Sejdinovic, D., Dolan, R. & Dayan, P. Temporal structure in associative retrieval. *Elife* **4**, e04919 (2015)

16. Kurth-Nelson, Z., Economides, M., Dolan, R. J. & Dayan, P. Fast Sequences of Non-spatial State Representations in Humans. *Neuron* **91**, 194–204 (2016)

17. Hunt, L. T. *et al*. Mechanisms underlying cortical activity during value-guided choice. *Nat. Neurosci.* **15**, 470–476 (2012)

18. Hotelling, H. Relations between two sets of variates. *Biometrika* **28**, 321–377 (1936).

19. Simon, H. A. *Models of bounded rationality: Empirically grounded economic reason* (MIT press., 1982)

20. Howes, A., Vera, A., Lewis, R. L. & McCurdy, M. Cognitive constraint modeling: A formal approach to supporting reasoning about behavior. In: *Proceedings of the 26th Annual Meeting of the Cognitive Science Society,* 595–600 (Hillsdale, NJ, Lawrence Erlbaum, 2004)

21. Wickelgren, W. A. Speed-accuracy tradeoff and information processing dynamics. *Acta Psychol.* **41**, 67–85 (1977)

22. Krajbich, I., Armel, C. & Rangel, A. Visual fixations and the computation and comparison of value in simple choice. *Nat. Neurosci.* **13**, 1292–1298 (2010)

23. Dai, J. & Busemeyer, J.R. A probabilistic, dynamic, and attribute-wise model of intertemporal choice. *J. Exp. Psychol. Gen.* **143**, 1489–1514 (2014)

24. Rich, E. L., & Wallis, J. D. Decoding subjective decisions from orbitofrontal cortex. *Nat. Neurosci*. **19**, 973–980 (2016)

25. Townsend, J. T., & Wenger, M. J. The serial-parallel dilemma: A case study in a linkage of theory and method. *Psychon. B. Rev.*, **11**, 391–418 (2004)

26. Sternberg, R. J. & Grigorenko, E. L. Are cognitive styles still in style? *Am. Psychol.* **52**, 700 (1997)

27. Rayner, S. & Riding, R. Towards a categorisation of cognitive styles and learning styles. *Educ. Psychol.* **17**, 5–27 (1997)

28. Nisbett, R. E., Peng, K., Choi, I. & Norenzayan, A. Culture and systems of thought: holistic versus analytic cognition. *Psychol. Rev.* **108**, 291 (2001)

29. Felder, R. M., & Spurlin, J. Applications, reliability and validity of the index of learning styles. *Int. J. Eng. Educ.* **21**, 103–112 (2005)

30. Choi, I., Koo, M. & Choi, J. A. Individual differences in analytic versus holistic thinking. *Pers. Soc. Psychol. B.* **33**, 691–705 (2007)

31. Kozhevnikov, M. Cognitive styles in the context of modern psychology: toward an integrated framework of cognitive style. *Psychol. Bull.* **133**, 464 (2007)

32. Eldar, E., Cohen, J. D. & Niv, Y. The effects of neural gain on attention and learning. *Nat. Neurosci.* **16**, 1146–1153 (2013)

33. Montague, P. R., Dolan, R. J., Friston, K. J. & Dayan, P. Computational psychiatry. *Trends Cogn. Sci.* **16**, 72–80 (2012)

34. Wang, X. J. & Krystal, J. H. Computational psychiatry. *Neuron* **84**, 638–654 (2014)

35. Eldar, E. & Niv, Y. Interaction between emotional state and learning underlies mood instability. Nat. Commun. **6**, 6149 (2015)

36. Eldar, E., Hauser, T. U., Dayan, P. & Dolan, R. J. Striatal structure and function predict individual biases in learning to avoid pain. *Proc. Natl. Acad. Sci. USA* **113**, 4812–4817 (2016)

37. Schwarz, G. Estimating the dimension of a model. *Ann. Stat.* **6**, 461–464 (1978).

38. Bishop, C. M. *Pattern Recognition and Machine Learning* (Heidelberg, Germany, Springer, 2006)

39. Kass, R. E. & Raftery, A. E. Bayes factors. *J. Am. Stat. Assoc.* **90**, 773–795 (1995)

40. Huys, Q. J. *et al*. Bonsai trees in your head: how the Pavlovian system sculpts goal-directed choices by pruning decision trees. *PLoS Comp. Biol.* **8**, e1002410 (2012)

41. Oostenveld, R., Fries, P., Maris, E. & Schoffelen, J. M. FieldTrip: open source software for advanced analysis of MEG, EEG, and invasive electrophysiological data. *Comput. intel. Neurosci. 2011*, 156869 (2011)

42. Sun, L., Ji, S. & Ye, J. Canonical correlation analysis for multilabel classification: A least-squares formulation, extensions, and analysis. *IEEE T. on Pattern Anal.* **33**, 194–200 (2011)

43. Hoffman, K. L. & McNaughton, B. L. Coordinated reactivation of distributed memory traces in primate neocortex. *Science* **297**, 2070–2073 (2002)

44. Busch, N. & VanRullen, R. Is visual perception like a continuous flow or a series of snapshots. In: Arstila, V. & Lloyd. D. (Eds.) *Subjective time: The philosophy, psychology, and neuroscience of temporality* (MIT Press, 2014)

45. Maris, E. & Oostenveld, R. Nonparametric statistical testing of EEG-and MEG-data. *J. Neurosci. Meth.* **164**, 177–190 (2007)

46. Kessels, R. P., Van Zandvoort, M. J., Postma, A., Kappelle, L. J. & De Haan, E. H. The Corsi block-tapping task: standardization and normative data. *Appl. Neuropsychol.* **7**, 252–258 (2000)

47. Wechsler, D. & Hsiao-pin, C. *WASI-II: Wechsler abbreviated scale of intelligence* (Pearson, 2011)

48. Hoekstra, R. A. *et al*. The construction and validation of an abridged version of the autism-spectrum quotient (AQ-Short). *J. Autism Dev. Disord.* **41**, 589–596 (2011)

49. Kessler, R. C. *et al*. The World Health Organization Adult ADHD Self-Report Scale (ASRS): a short screening scale for use in the general population. *Psychol. Med.* **35**, 245–256 (2005)

Figure Captions

Fig. 1. Task design, performance, and model. n=40 participants. (**a**) Experimental stimuli comprised four types of players, each with a different scoring ability. (**b**) Participants had to determine the total number of goals each team of players would score. Participants were given either 1 or 2 s deliberation time before being prompted to report their decision. See **Supplementary Fig. 1** for pre-task training procedure. (**c**) Performance as a function of problem complexity and time. Participants were more likely to answer correctly for teams with fewer player types (p<0.001, β= –0.56, 95% CI: –0.63 to –0.49) and fewer players (p < 0.001, β= –0.24, 95% CI: –0.28 to –0.20), and when more time was available (p<0.001, β=0.25, 95% CI: 0.15-0.36; Boostrap test of multiple logistic regression coefficients). Dashed line: chance performance. Error bars: s.e.m. (**d**) Performance as a function of experimental block and time sensitivity. Participants were divided into time-sensitive (above median) and time-insensitive (below median) groups based on the increase in performance with deliberation time. (**e**) Performance on 1s trials as a function of problem complexity. Participants are ordered by sensitivity to complexity, computed as the performance dropoff in 1s trials with 4 player types compared to 1s trials with 1 player type. (**f**) Sensitivity to time as a function of sensitivity to complexity (robust estimation of regression coefficient for the z-scored measures, tested with random permutations: p=0.004, β=0.47, 95% CI: 0.20-0.75). (**g**) Participants' real answers (left) and those simulated by the best-fitting computational model (right), shown in terms of average error. Error bars: s.e.m. across subjects, and 95% CI across 1000 model simulations. (**h**) The model's computation of players' scoring as function of resource allocation, for a trial with 3 players of each

39

type. (**i**) Model's resource allocation as function of player and trial type. (**j**) Model's prioritization: prioritizing higher-scoring (top), more numerous (left), or centrally-located (right) players. Numbers: log Bayes factors compared to uniform division of resources. See **Supplementary Fig. 2** for additional models. (**k,l**) Computational precision with maximal resources relative to minimal resources, estimated by model parameter ω, as a function of sensitivity to time (**k**; p=0.01, β=0.50, 95% CI: 0.19-0.81) and complexity (**l**; p=0.03, β=0.46, 95% CI: 0.15-0.76; robust estimation of regression coefficient for the z-scored measures, tested with random permutations). Y axes are logarithmic.

Fig. 2. Cortical representations of the players composing a team. n=40 participants. Participants are divided into high and low sensitivity groups (i.e. above and below median) using a combined measure of time and complexity sensitivity that equally weighs the two z-scored measures of sensitivity from **Fig. 1**f. (**a**) Correlation between actual and decoded numbers of players, averaged across player types. As a control, we also show the correlation between the actual and decoded numbers of different players. Decoders were trained on all time points in the preliminary task from 150ms following stimulus onset (see **Supplementary Fig. 5**). Chance decoding corresponds to zero correlation. (**b**) 'Sequenceness'[16] between representations of players of different types, with types ordered from high to low priority, as inferred using the model (see **Fig. 1**). Sequenceness was computed for all player type pairs within a trial, and for all time lags between 0 to 0.2 s separating the player types. Results were averaged over time lags, pairs and trials. The X axis indicates mean trial time from which the first of each pair of player types was decoded. Permutation test of sum of t-values comparing between high and low sensitivity groups across timepoints: $\sum t$=116.5, df =38, p=0.01, M=0.0079, extent: 37 timepoints. ●: significant difference from zero, ◆: significant difference between groups. Significance tests accounted for multiple comparions by means of a permutation test: we conducted a separate t test for each time point, and we deemed significant stretches of consecutive time points with $p_{\text{uncorrected}}$ < 0.05 over which the sum of t values exceeded the maximal
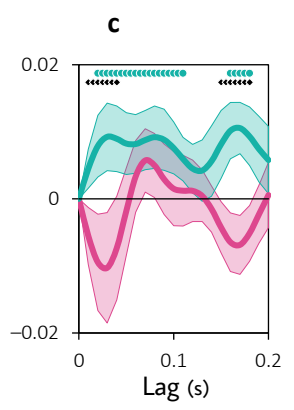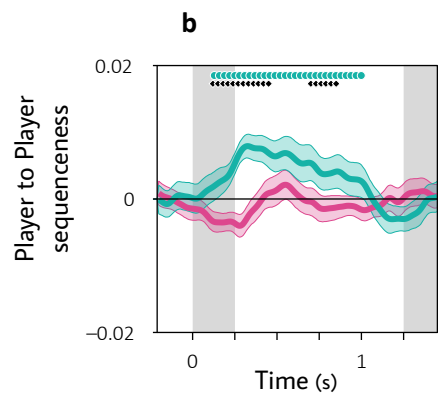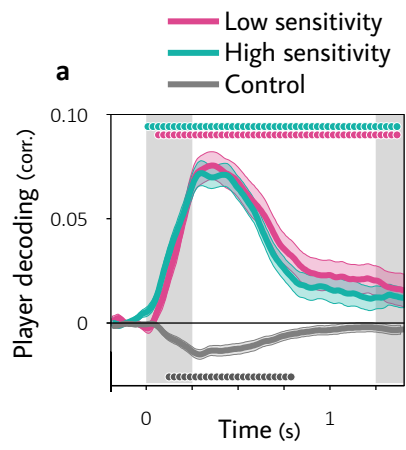
sum-of-t obtained with 95% of random permutations of the data (see **Time-series analyses** in the

Methods for further details). Colored areas: s.e.m. (**c**) Player-to-player 'sequenceness', computed as

in panel (**b**), but averaged over the duration of the trial and shown as a function of time lag between

player types. In all panels, gray areas indicate when players were presented on the screen

(beginning) and the time participants were prompted to report their decision in 1s trials (end). The

results include both 1s and 2s trials, with data from 2s trials truncated to fit the plot.
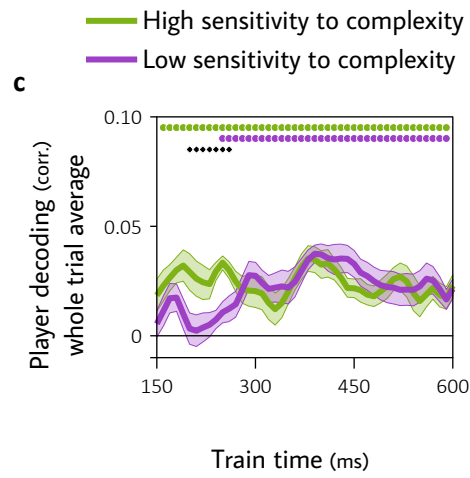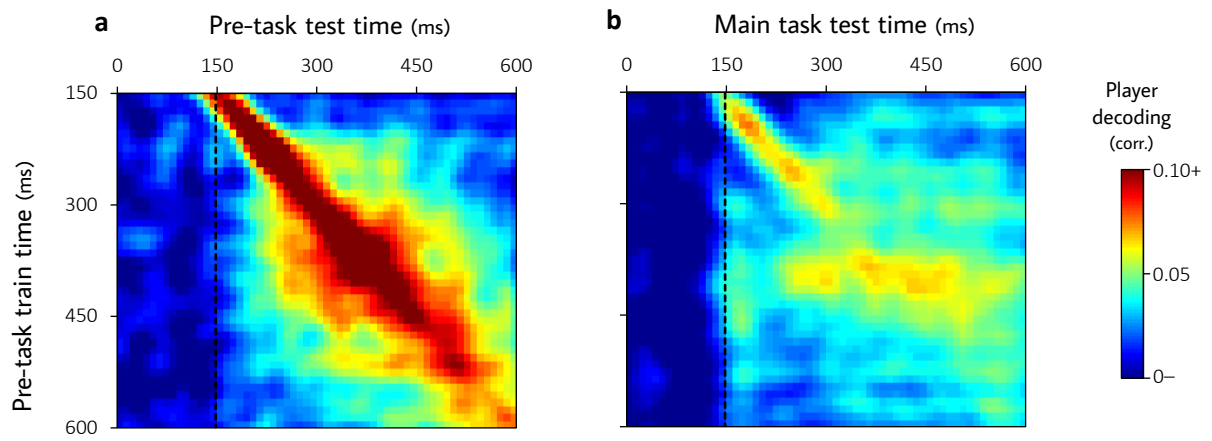

Fig. 3. Temporal components of the neural response. n=40 participants. (**a**) Decoding performance in

the preliminary task as a function of training and testing time. Performance was computed as the

correlation between actual and decoded quantities as in **Fig. 2**. Players were represented in a largely

time-point-specific manner. Training and testing trials were kept separate using 5-fold cross

validation. (**b**) Decoding performance in the main task as a function of training and testing time.

Decoders were trained on data from the preliminary task and tested on data from the main task. In

panels **a** and **b**, the dashed line marks the testing time point corresponding to the earliest

component training time (150ms). (**c**) Main task decoding performance as a function of training

time. Participants were divided into high and low sensitivity-to-complexity groups, 19 participants

each, based on a median split on the behavioral measure from **Fig. 1**e. Permutation test of sum of t-

values comparing between the groups across timepoints: $\sum t$=21.2, df=36, p=0.02, M=0.02, extent: 8

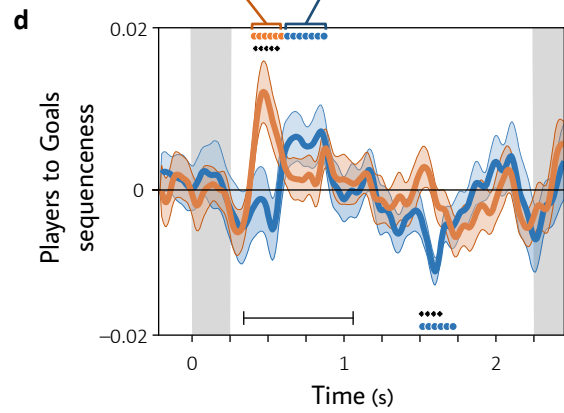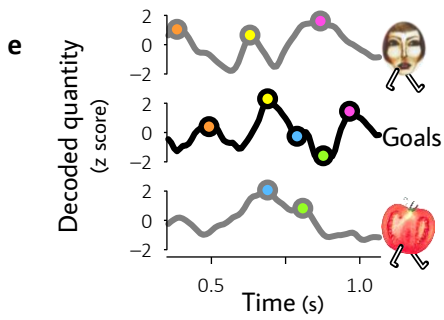components. •: difference from zero, ♦: difference between groups ($p < 0.05$). Shaded areas: s.e.m.
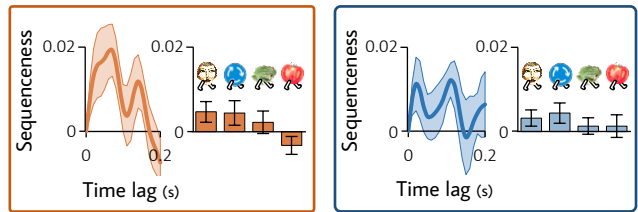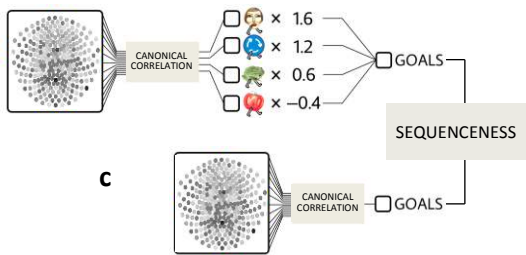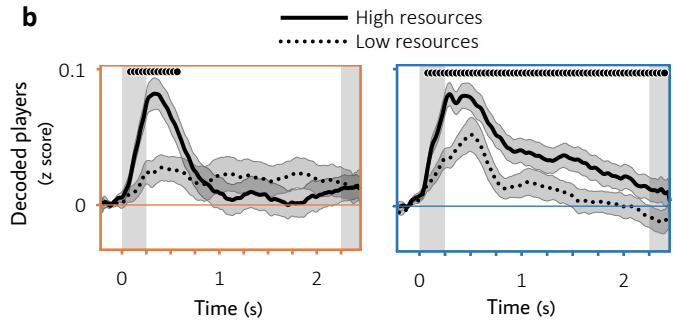

Fig. 4. Cortical representation of players and goals in 2 s trials. n=40 participants. (**a**) Correlation

between actual and decoded numbers of players, averaged across player types, for time-insensitive

($\sum t$=342.3, df=19, p=0.02, M=0.05, extent: 57 timepoints) and time-sensitive ($\sum t$=1112.0, df=19,

p<0.001, M=0.04, extent: 200 timepoints; permutation test of sum of t-values across timepoints)

participants. (**b**) Influence of resource allocation on cortical representations. Decoded player

quantities weighted by players' optimally ('High resources') and minimally ('Low resources') processed components, as inferred from participants' decisions using the model (s_+ and s_-), for time-insensitive (left) and time-sensitive (right) participants. To isolate the effect of resource allocation, variance associated across trials with the actual number of players of a given type was removed from its decoded quantities using linear regression. (**c**) We examined the sequential relationship ('sequenceness'[16]) between the number of goals that corresponds to represented players (a sum of decoded player quantities multiplied by player scoring abilities) and a directly decoded prediction of the number of goals the participant eventually decided on. (**d**) Players-to-goals sequenceness as function of time sensitivity. The X axis indicates mean trial time from which the players were decoded. Insets show statistically significant stretches of sequenceness broken down by time lag between players and goals (line plot) and player type (bars show player-to-goals sequenceness computed on each player's quantity without multiplying by scoring ability). Bottom bar indicates timing of example timeline shown in panel **e**. Permutation test of sum of t-values comparing between the groups across timepoints: $\sum t$=35.4, df=38, p=0.01, M=0.01, extent: 15 timepoints (**e**) Example timeline of decoded players and predicted answer, demonstrating the dynamics captured by the 'sequenceness' measure in (**c,d**). Every increase in the representation of faces (1.6 goals per game) is followed by an increase in the decoded number of goals, while increases in the representation of tomatoes (minus 0.4 goals per game) are followed by goal decreases. For clarity, face and tomato peaks and subsequent changes in the decision signal are marked with matching colors. In all panels, •: significant difference from zero (**a,d**) or from 'min resources' (**b**), ◆: significant difference between time-insensitive and time-sensitive groups (permutation test: p<0.05). Gray areas indicate trial events as in **Fig. 2**. Error bars and colored areas: s.e.m.

a

Goals per game

(face)	1.6
(blue)	1.2
(artichoke)	0.6
(tomato)	minus 0.4

b

½ – 1 s

¼ s

1 or 2 s

variable

How many goals will the team score?

Time

c

Correct decisions

Players 1 — 12

100%

50%

0%

1s 2s · 1s 2s · 1s 2s · 1s 2s

1 · 2 · 3 · 4

Player types

d

Correct decisions

60%

40%

20%

0%

1 2 3 4 5 6 7

Experimental block

○ 1 second
△ 2 seconds
■ Time insensitive
■ Time sensitive

e

■ 1 player type
■ 2/3 player types
■ 4 player types

1s correct decisions

100%

50%

0%

0 20 40

Participant

f

Sensitivity to time

20%

10%

0%

–10%

20% 60% 100%

Sensitivity to complexity

g

REAL   SIMULATED

Error (goals)

1

0

–1

–2

–3

0 1 2 3 4 5 6 7 8 9 10   0 1 2 3 4 5 6 7 8 9 10

Correct number of goals

— 1 player type
— 2 player types
— 3 player types
— 4 player types

h

Computed scoring

1.5

1.0

0.5

0

–0.5

Min   Max

Allocated recources

i

Average resource allocation

Max

Min

player types
○ 1 ● 2 ● 3 ● 4

j

146

170   168

177

18   10

28

k

Relative precision with max resources (ω)

100

10

1

–10% 0% 10% 20%

Sensitivity to time

l

Relative precision with max resources (ω)

100

10

1

20% 60% 100%

Sensitivity to complexity

a Pre-task test time (ms)

b Main task test time (ms)

Player decoding (corr.)

c

High sensitivity to complexity

Low sensitivity to complexity

Player decoding (corr.) whole trial average

Train time (ms)

a

Time insensitive
Time sensitive

b

High resources
Low resources

c

CANONICAL CORRELATION → GOALS

× 1.6
× 1.2
× 0.6
× −0.4

GOALS

SEQUENCENESS

d

e

Goals

MEG decoding reveals structural differences
within integrative decision processes

Eran Eldar[1,2], Gyung Jin Bae[1,2], Zeb Kurth-Nelson[1,2], Peter Dayan[2,3], Raymond J. Dolan[1,2]

[1] Wellcome Trust Centre for Neuroimaging, University College London, London WC1N 3BG, UK
[2] Max Planck University College London Centre for Computational Psychiatry and Ageing Research, London WC1B 5EH, UK
[3] Gatsby Computational Neuroscience Unit, University College London, London W1T 4JG, UK

Supplementary Information

Contents:

a

Block	Player types	Player types in a team	Trials	Performance criterion
1	1.6	1	12.5 ±0.7	8
2	1.6, 1.2	1	12.5 ±0.5	5 for each type
3	1.6, 1.2, 0.6	1	20.0 ±1.1	5 for each type
4	all	1	28.8 ±1.2	5 for each type
5	all	2	25	none
6	all	3	25	none

b
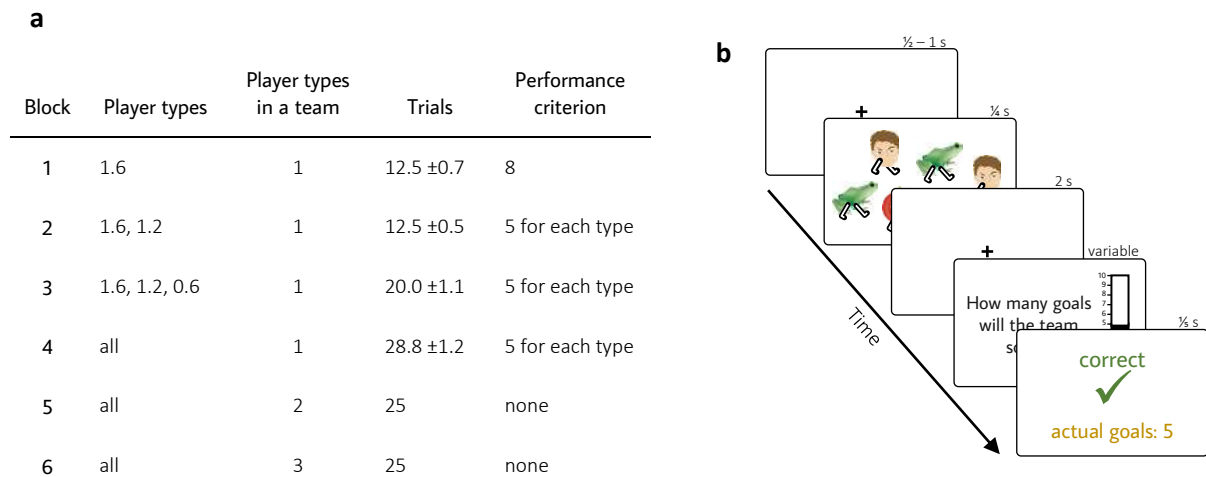
Supplementary Fig. 1. Training. (**a**) Participants performed 6 blocks of training trials, progressing gradually from the highest to the lowest scoring player, and then to teams with multiple player types. Training on teams with a single player type continued until the participant reached a certain score ('performance criterion'). 1 point was awarded for each correct decision, and ½ point was deducted when a decision differed from the correct number by more than one goal. (**b**) Timeline of one training trial. Trials progressed similarly to 2 s trials in the main task, except that feedback was provided after each decision.
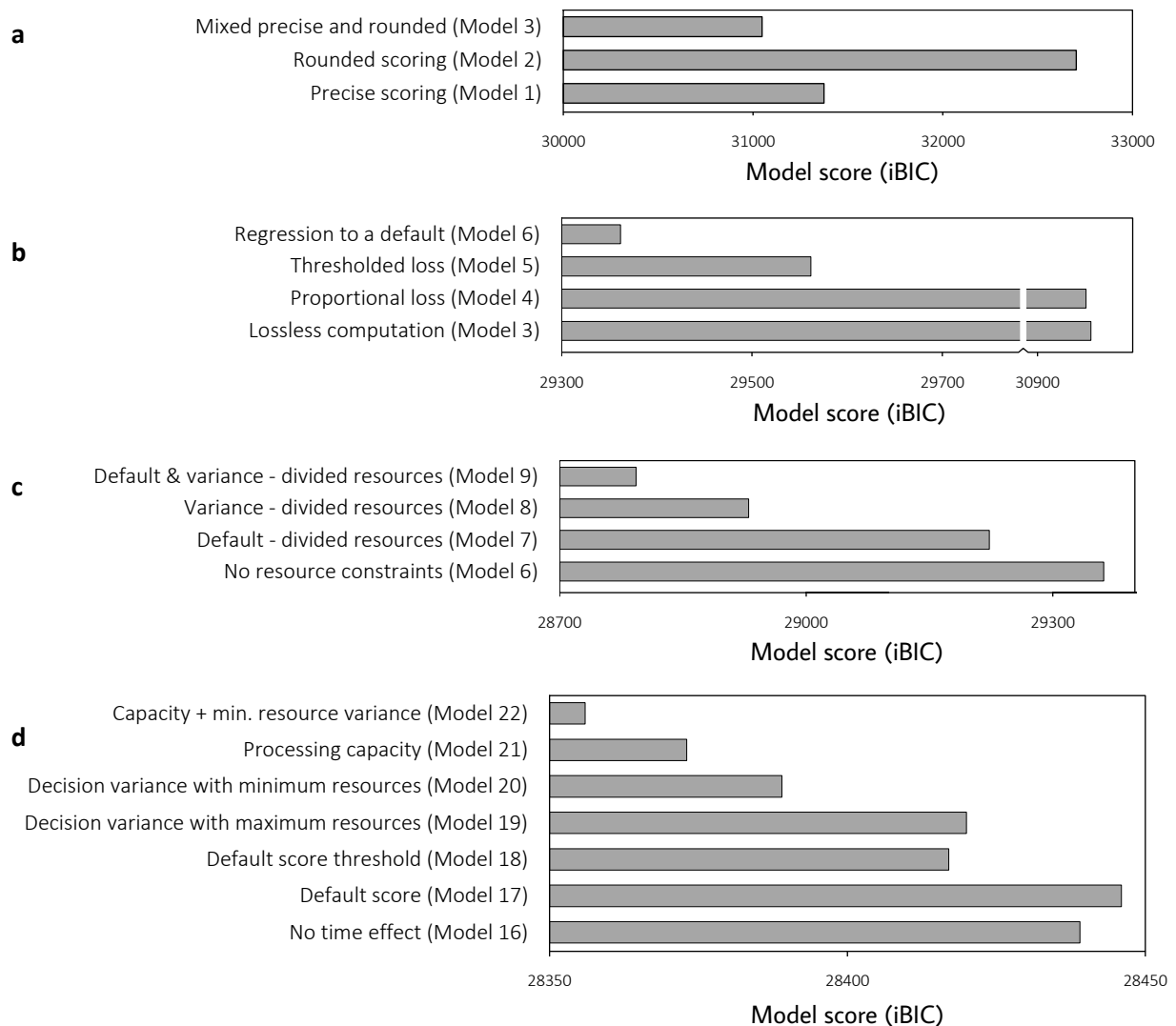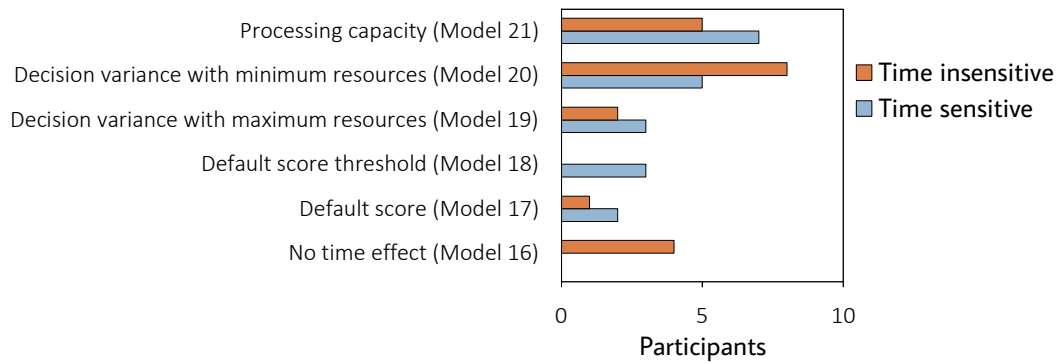
Supplementary Fig. 2. Modeling participants' decisions. n = 40 participants. To gain further insight into participants' decision processes we compared multiple models in terms of how well they explained participants' decisions in the task. The panels show successive stages of development of the model, where in each stage we compared between multiple variants of the best-fitting model from the next stage. Lower iBIC score (integrated Bayesian Information Criterion) indicates better fit with participants' decisions (see **Methods** for details of all models and model comparison procedure). (**a**) We first tested whether participants based their decision on the players' precise scoring abilities, on the closest integer number ('Rounded scoring'), or on a linear combination of the two ('Mixed precise and rounded'). (**b**) We then tested whether participants took into account all players ('Lossless computation' – the best-fitting model from (**a**)), ignored some proportion of the players ('Proportional loss' and 'Thresholded loss'), or accounted for these players via a default value that ignores player type ('Regression to a default'). (**c**) Thirdly, we tested whether participants' decisions were better explained by assuming that processing resources had to be divided between players that appeared together. To this end, we compared the best-fitting model from (**b**), termed here 'No resource constraint', to models in which resources were divided between players, determining how precisely they were computed ('Variance'), how likely they were to be accounted for via a default value ('Default'), or both ('Default & variance'). (**d**), After finding how participants prioritized players with respect to one another (see **Fig. 1**j), we tested how performance differences between 1 s and 2 s trials could best be explained. To this end, we compared the best-fitting model from **Fig. 1**j, termed here 'No time effect', to models in which longer time for deliberation allowed a higher default value ('Default score'), a higher threshold beyond which players were accounted for via the default value ('Default score threshold'), lower decision variance in the computation of players that were allocated maximum or minimum resources, greater processing resources allocation ('Processing capacity'), and finally, a combination of the two factors for which we found considerable evidence ('Capacity + min. resource variance').

a

b
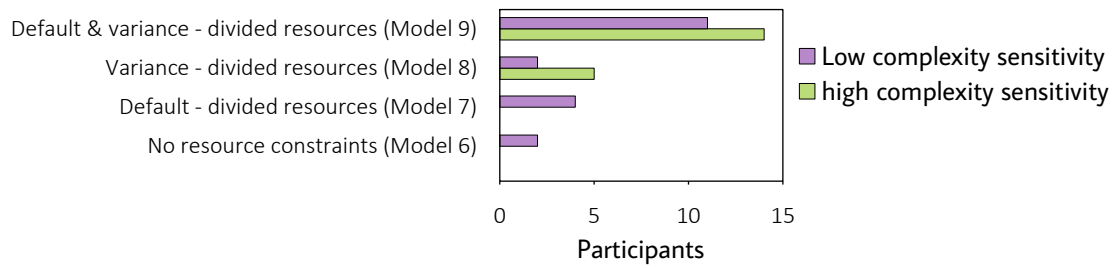
Supplementary Fig. 3. Model comparisons testing the effects of time and complexity on participants' answers. (**a**) Best-fitting model for participants with low and high sensitivity to complexity. This model comparison tests whether the effect of problem complexity can be explained as reflecting a division of processing resources (see **Supplementary Fig. 2**c). (**b**) Best-fitting model for time-sensitive and time-insensitive participants. This model comparison tests different possible effects of additional time for deliberation (see **Supplementary Fig. 2**d). The best-fitting model overall (Model 22; see **Methods**) combines Model 20 and Model 21. In both panels, participants are divided using a median split on the sensitivity measures from **Fig. 1**h.

a

b
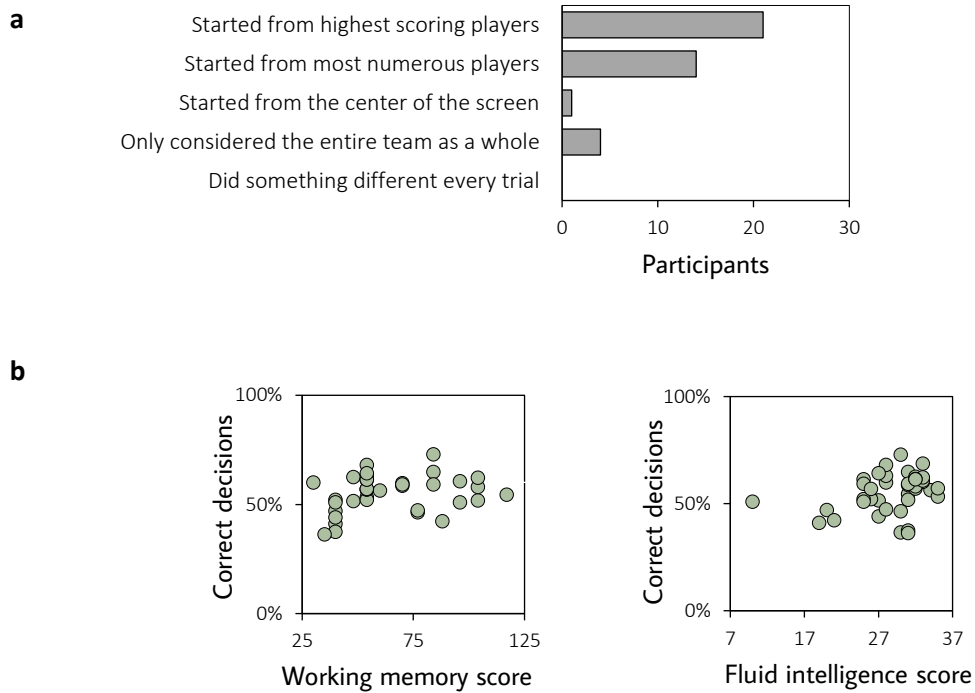
Supplementary Fig. 4. Independent measures of individual differences. n = 40 participants. (**a**) Participant reports following the experiment. Participants were asked to describe how they reached decisions in the task by choosing one of the five answers shown on the Y axis. (**b**) Overall performance in the task as a function of working memory capacity (left; $p_{permutation}$ = 0.06, β_{robust} = 0.31, 95% CI: −0.01 to 0.64) and fluid intelligence (right; $p_{permutation}$ = 0.04, β_{robust} = 0.36, 95% CI: 0.05 to 0.66). No other independent measure correlated with task performance. Working memory was measured as the total score on a Corsi Block test[1]. Fluid intelligence was measured using the matrix reasoning component of the Wechsler Abbreviated Scale of Intelligence[2].
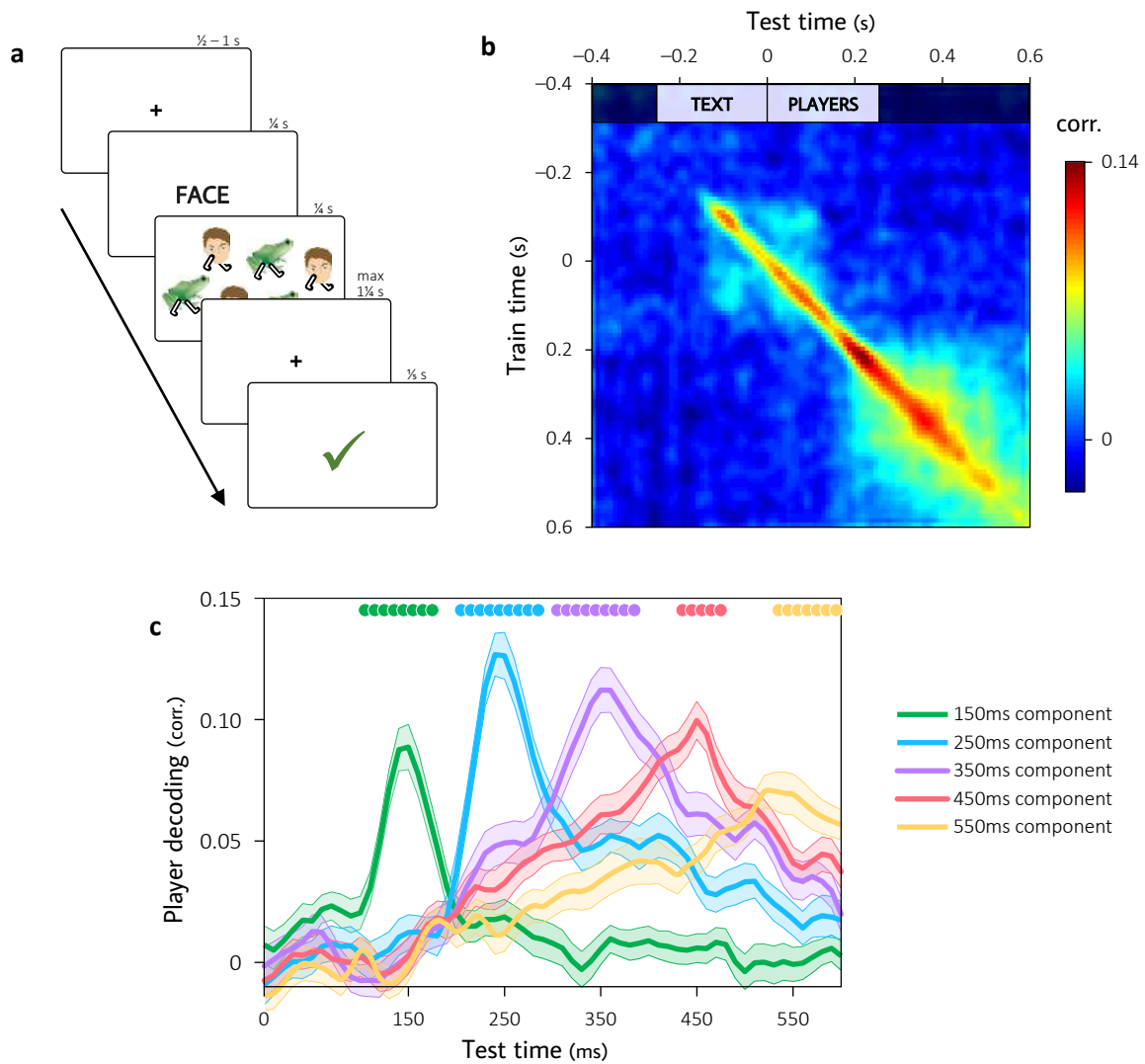
Supplementary Fig. 5. Construction of the MEG decoder. n = 40 participants. (**a**) Timeline of one trial. Before the main task, participants were asked to count the number of players corresponding to a word (e.g., 'FACE') that appeared on the screen 250 ms before the players. Trials continued until participants completed at least 30 successful trials with each of 6 player types (mean 202 ±2 trials). Similarly to the main task, players were presented for 250 ms. Participants were given a maximum of 1.5 s to respond (median response time was 666 ±14 ms). Feedback ('✓' or 'X') was given immediately following response. (**b**) MEG decoder performance. We used the MEG spatial pattern from each 10 ms time bin ('Train time') to train a canonical correlation decoder to predict the number of players the participant was counting of each player type. We then tested the 101 resulting decoders by applying them to each 10 ms time bin ('Test time') in a separate subset of trials not used for training (i.e., via 5-fold cross validation). Decoding performance, computed as the correlation between actual and decoded quantities, is shown for each pair of time bins. Correlations were computed separately for each player type and then averaged. Decoding was successful from 110 ms after text onset (plot diagonal is significantly positive between –0.14 s and 0.6 s, $p < 10^{-5}$, permutation test). Players were represented in MEG in a largely time-point-specific manner, as indicated by the diagonal ridge that apparent in the plot. Decoding accuracy sharply increased further 150 ms following players onset, presumably indicating the time point participants began to identify players in the visual display. This was similar in participants later labeled as time-insensitive (160 ms) and time-sensitive (150 ms), and in both groups decoding was successful throughout the remainder of the trial. We thus used the models trained on time bins between 150 and 600 ms following players onset to detect player representations in the main task. (**c**) Decoding performance for five different training times as a function of testing time. ●: significantly higher than any other component ($p_{permutation} < 0.05$).
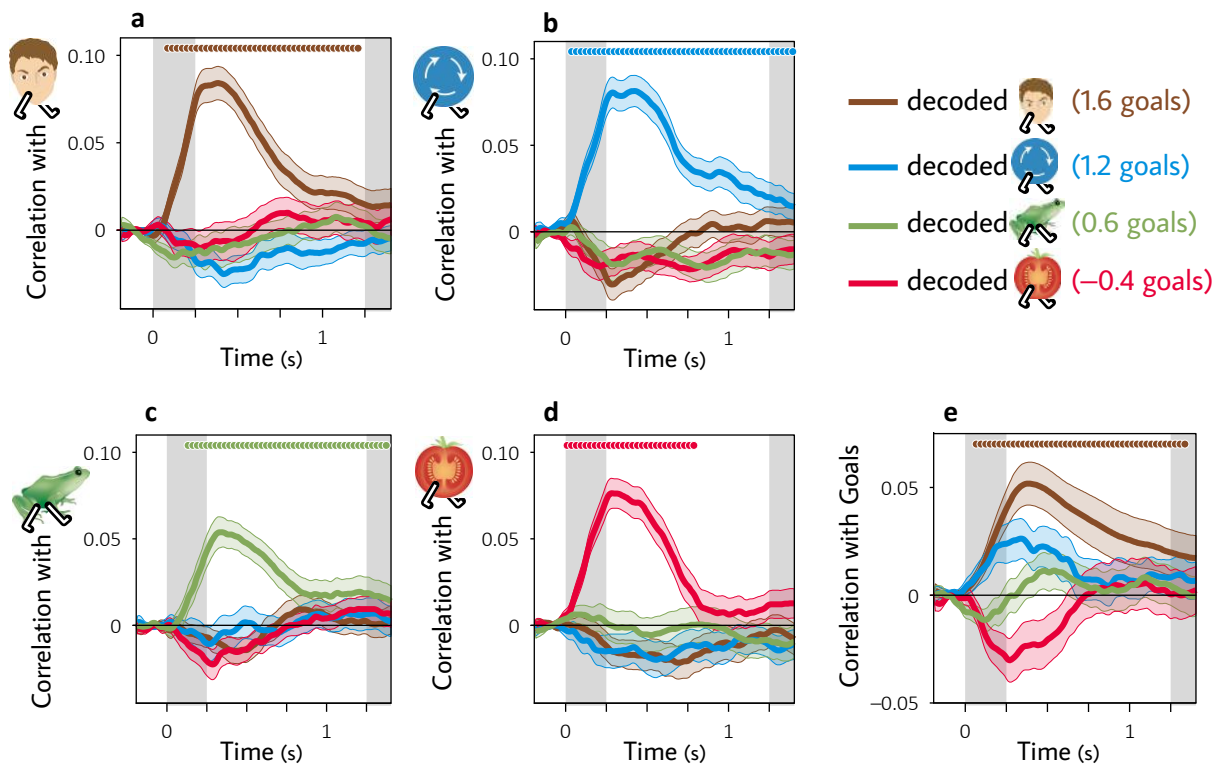
Supplementary Fig. 6. Correlations of decoded and actual quantities. The five plots show the correlation, across trials, between the decoded quantities of each player type during the main task, and the actual number of (**a**) highest scoring player, (**b**) 2nd highest scoring player, (**c**) 3rd highest scoring player, (**d**) negative scoring player, and (**e**) the number of goals the participant chose. ●: difference from zero ($p_{permutation} < 0.05$). The results include both 1s and 2s trials, with data from 2s trials truncated to fit the plot.
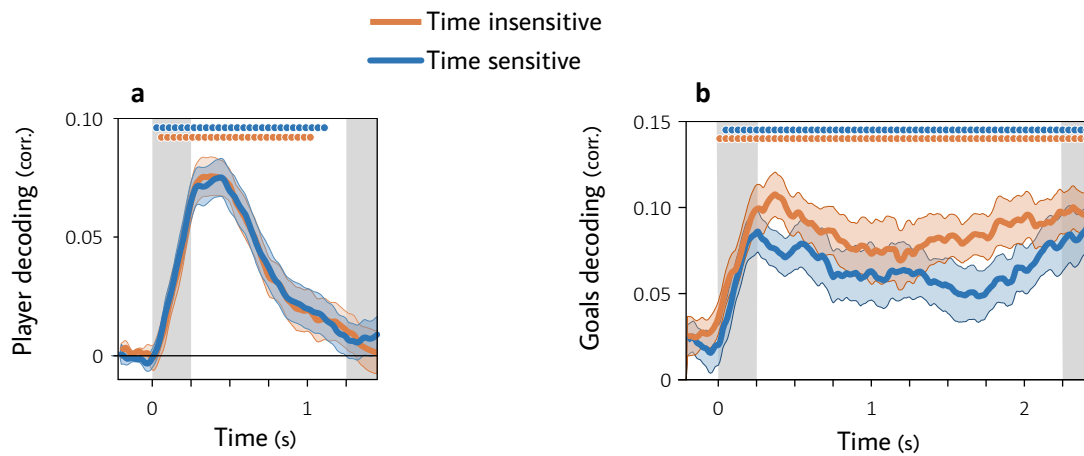
Supplementary Fig. 7. Cortical representations during task performance. *n* = 40 participants. (**a**) Representation of players in 1s trials. The plot shows the correlation between actual numbers of players and player quantities decoded from MEG, averaged over player types. (**b**) Representation of eventual decisions in trials with multiple player types. The plot shows the correlation between the number of goals participants actually decided on and the decision decoded from MEG. ●: difference from zero ($p_{\text{permutation}} < 0.05$). Gray areas: trial events as in **Fig. 2**. Colored areas: s.e.m.
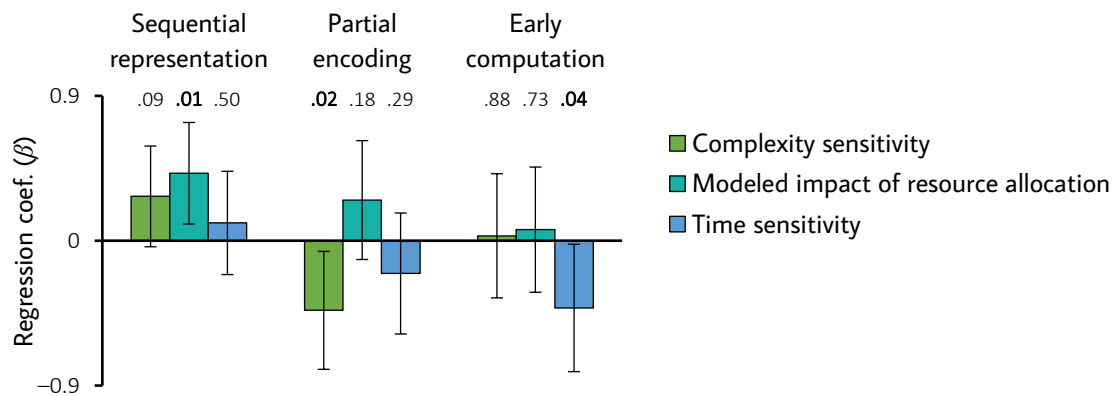

Supplementary Fig. 8. MEG indices and behavioral measures of sensitivity to time and complexity. 'Sequential representation' refers to player-to-player sequenceness averaged over the entire duration of the trial (see **Fig. 2**b). 'Partial encoding' refers to a mean of temporal components of the neural response weighted by decoding accuracy (see **Fig. 3**c). 'Early computation' refers to an average of the earliest significant cluster of players-to-goals sequenceness from **Fig. 4**d. Each feature was regressed on the different types of sensitivity in separate linear robust regression model, for which all quantities were *z*-scored. Numbers indicate p values produced by the regression model (bold: <0.05). Error bars: 95% CI. Sensitivities were computed as in **Fig. 1**f, with the modeled impact of resource allocation corresponding to model parameter ω.
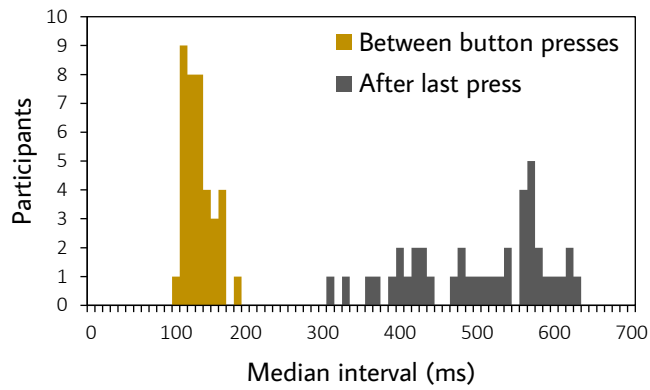
Supplementary Fig. 9. Median time intervals between participants' button presses, and time left for entering one's answer after the last button press.
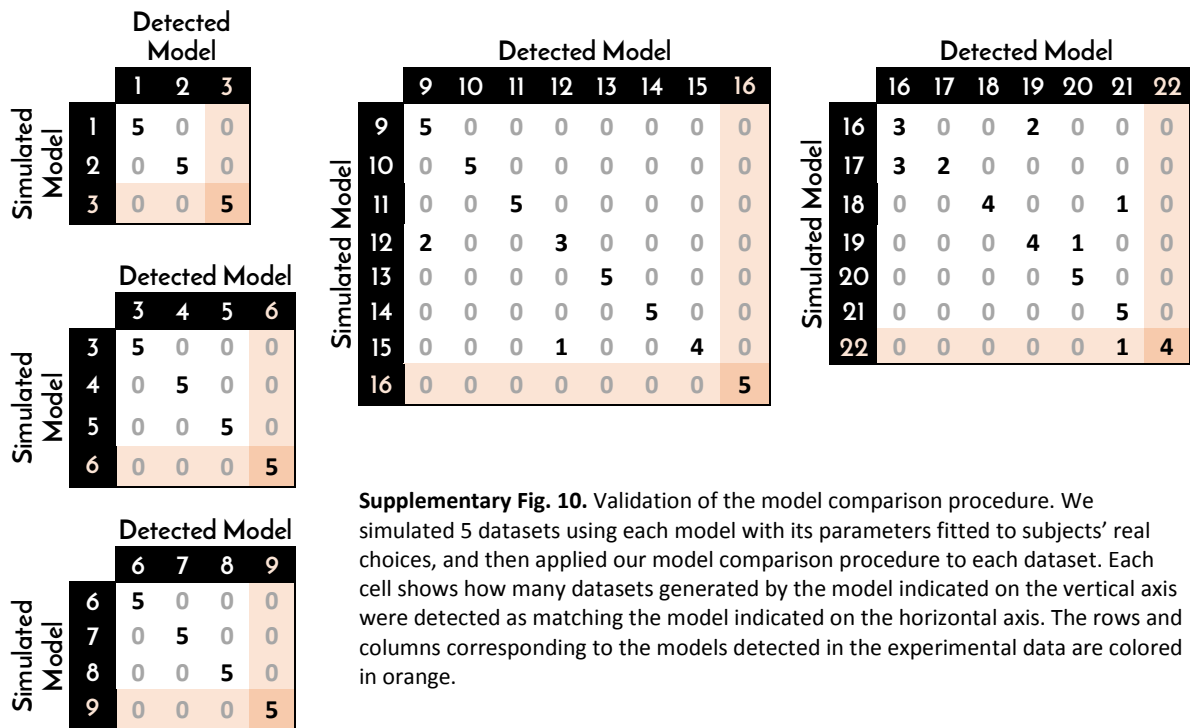
Supplementary Fig. 10. Validation of the model comparison procedure. We simulated 5 datasets using each model with its parameters fitted to subjects' real choices, and then applied our model comparison procedure to each dataset. Each cell shows how many datasets generated by the model indicated on the vertical axis were detected as matching the model indicated on the horizontal axis. The rows and columns corresponding to the models detected in the experimental data are colored in orange.
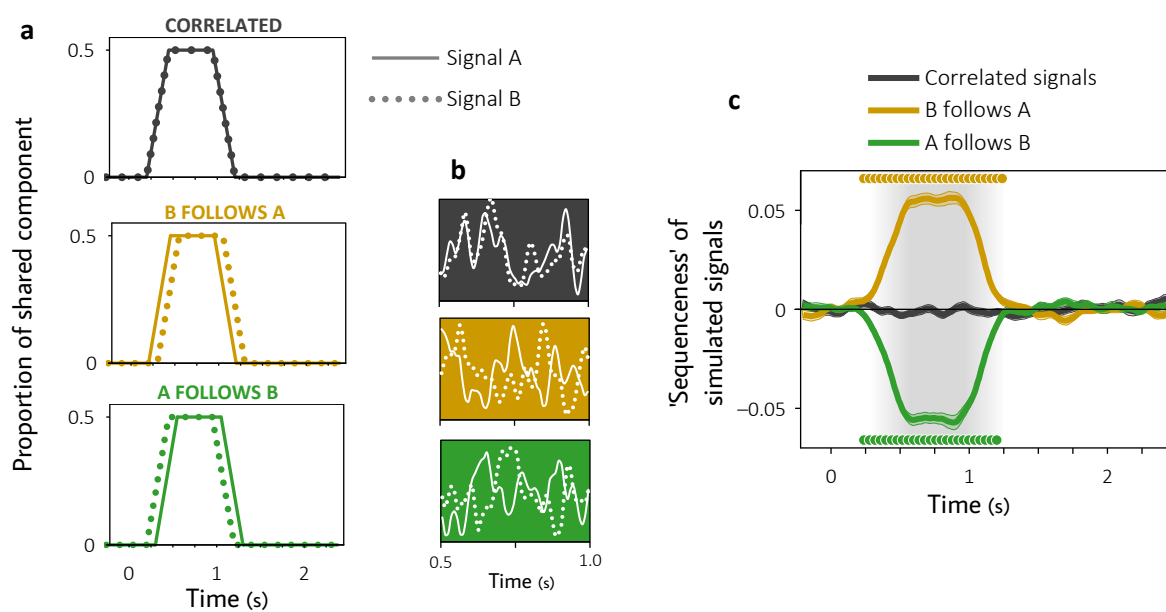
Supplementary Fig. 11. Validation of 'sequenceness' analysis. (**a**) We simulated three datasets, one with pairs of correlated signals ('correlated'), and two where the signals followed one another in time ('B follows A' and 'A follows B'). For each dataset, we generated pairs of random time series that matched the pairs of signals from the sequenceness analysis in **Fig. 4**d in terms of their power spectrum density (PSD; 'Signal A' matched the players-based time series and 'Signal B' matched the goals-based time series). Thus, one pair of signals was generated for each trial of each subject. To simulate dependency between the two signals, a portion of each pair (from the 250 ms to the 1250 ms mark) was partially replaced by a shared component with a similar frequency content. To minimize transition artifacts, the shared component was gradually mixed into and out of the signals over periods of 250 ms. For the 'correlated' dataset, the shared component was inserted at the same time points in Signal A and Signal B, whereas for the 'B follows A' dataset, the shared component was inserted into Signal B 200 ms later than for Signal A (and vice versa for the 'A follows B' dataset). (**b**) Example snippets of generated time series from each of the three color-coded datasets. (**c**) Sequenceness from Signal A to Signal B was computed as in **Fig. 4**d. Gray shading indicates where the signals shared a common component. Matched signals were created by generating white noise, multiplying it by a target signal's PSD, and applying inverse Fourier transform. ●: difference from zero ($p_{permutation} <$ 0.05). Color areas: s.e.m.
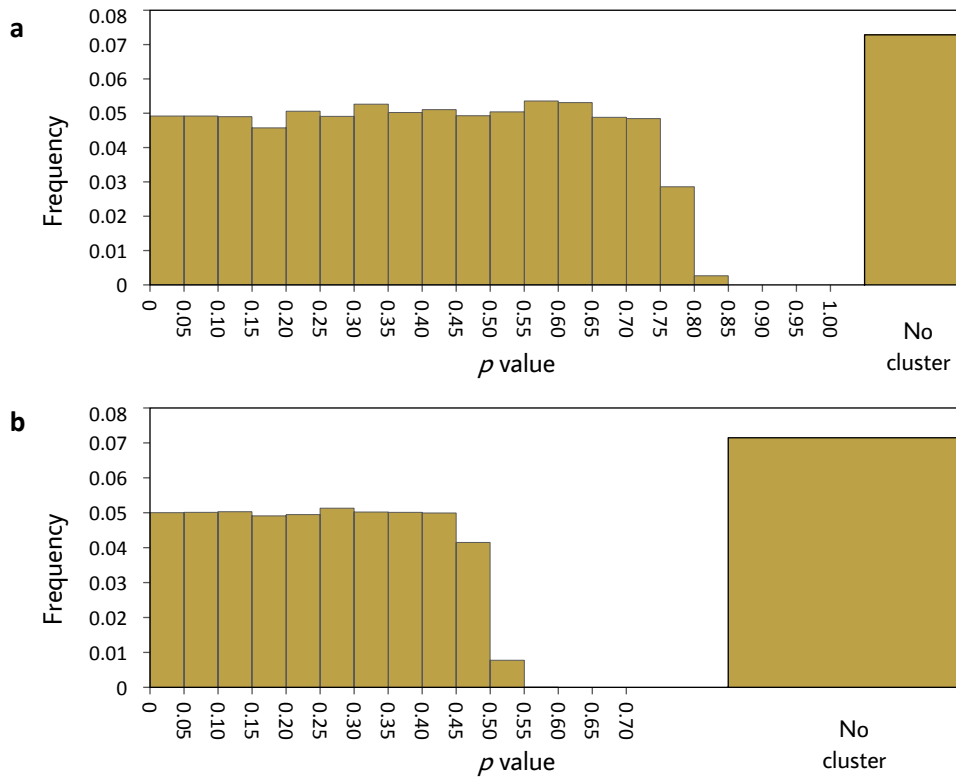
Supplementary Fig. 12. Validation of statistical tests for autocorrelated time series. (**a**) To validate our method of detecting significant differences from zero, we generated random time series matching all subjects' time series of player-to-goal sequenceness (see **Fig. 4**d), on a trial-by-trial basis, in terms of their intensity and correlation length. We then applied our permutation test method to detect clusters of timepoints that significantly differed from zero. This procedure was iterated 10,000 times. Significant clusters (p < 0.05) were detected in 0.05 of iterations. (**b**) To validate our method of detecting significant differences between groups, we again generated 10,000 datasets. Each dataset comprised random time series matching all subjects' time series of player-to-player sequenceness (see **Fig. 2**b). We then applied our permutation test method to detect clusters with significant difference between the low and high sensitivity groups. Significant clusters (p < 0.05) were detected in 0.05 of iterations. For both analyses, matching random time series were generated by computing the original time series' correlation length, creating a Gaussian filter accordingly, and convolving the filter with uncorrelated Gaussian noise[3].

PC 1 (63.8%)	1 type	2 types	3 types	4 types
2 seconds	0.27	0.56	0.40	0.26
1 second	0.26	0.46	0.30	0.10

PC 2 (12.9%)	1 type	2 types	3 types	4 types
2 seconds	-0.22	-0.21	-0.01	0.33
1 second	-0.12	-0.04	0.19	0.86

PC 3,4,5 (5.6%)	1 type	2 types	3 types	4 types
2 seconds	-0.06	0.19	0.17	0.29
1 second	-0.01	-0.38	-0.17	-0.06

Supplementary Table 1. Principal component analysis of the eight experimental conditions. The table shows the compositions of the first component ('PC 1'), which correlated with overall performance ($r = 0.99$, $p = 3×10^{-33}$; Pearson Correlation) and with combined sensitivity to time and complexity ($r = 0.42$, $p = 0.007$); the second component ('PC 2'), which correlated most strongly with complexity sensitivity ($r = 0.85$, $p = 3×10^{-12}$); and an average of the third, fourth and fifth components ('PC 3,4,5'), which correlated most strongly with time sensitivity ($r = 0.71$, $p = 4×10^{-7}$). Percentages indicate proportion of variance explained.

Supplementary References

1. Kessels, R. P., Van Zandvoort, M. J., Postma, A., Kappelle, L. J. & De Haan, E. H. The Corsi block-tapping task: standardization and normative data. Appl. Neuropsychol. 7, 252–258 (2000)

2. Wechsler, D. & Hsiao-pin, C. WASI-II: Wechsler abbreviated scale of intelligence (Pearson, 2011)

3. Garcia, N. & Stoll, E. Monte Carlo calculation for electromagnetic-wave scattering from random rough surfaces. *Phys. Rev. Lett.* 52, 1798–1801 (1984)